N. Jb. Miner. Abh.
2007, Vol. 183/3, p. 227–249, Stuttgart, April 2007, published online 2007

The Lavrion deposit (SE Attica, Greece): geology, mineralogy and minor elements chemistry

Nikos Skarpelis, Athens

With 12 figures, 4 tables and 1 appendix

Abstract: In southeastern Attica the Cycladic "Blueschist" and the "Basal" units are superposed and separated by a detachment fault. The widespread carbonate-hosted massive sulfide Pb–Zn–Ag ores of Lavrion are spatially related to the detachment fault, shear bands within marbles, and the shear contact between marbles and the intercalated metaclastics of the Basal Unit. The ores are both structurally and lithologically controlled. A low tonnage Ag-rich tension gash vein, hosted within hydrothermally altered hornfelses surrounding the Lavrion granodiorite, is structurally related to the regional stress field with roughly N–S direction. The ore mineral suite consists of base metal sulfides and a variety of sulfosalts and native elements. Galena and fahlore are the main silver carriers. There are no significant enrichments in minor elements other than Cd, Ag and Au. The sulfide mineral assemblages and the range of FeS compositions of sphalerite coexisting with pyrite, indicate an intermediate sulfidation state for the hydrothermal fluids generating the manto ores. Mineral assemblages characteristic of low or high sulfidation state are locally present. The ore geometry, structural and lithological control of the mineralization, textural features, carbonate alteration and silicification, and the mineralogic and chemical composition of the ores suggest a carbonate-replacement deposit affiliation.

Key words: mineralogy, manto, detachment, sulfides, sulfosalts, Miocene, Lavrion, Greece.

Introduction

The area of Lavrion in the SE part of Attica, is known as a center of silver and lead production. Exploitation started possibly 3.000 years ago. Mining flourished during the 5^{th}–4^{th} centuries B. C. It has been estimated that over 3500 t of silver and 1.4 Mt of lead had been produced during those centuries (Conofagos 1980). The fact that Athens had silver and lead resources had a fundamental bearing on Athens' rise to economic and cultural flourishing. Mining declined toward the end of the 3^{rd} century B. C. and revived during the Roman times. The Lavrion mines re-opened in 1866 and the exploited ore was processed mainly for recovery of silver, lead and zinc. Minor amounts of copper, speiss and fluorite were also produced (Marinos & Petrascheck 1956). As_2O_3 was produced from speiss during metallurgical processing of galena concentrates comprising native arsenic and As-bearing minerals. Part of mining during the 19^{th} and 20^{th} centuries A. D. was of supergene ore. Supergene non-sulfide Zn, Fe, Ag and Pb ores (Skarpelis 2004) were of significant economic importance. The mines closed permanently in 1978 due to exhaustion of economic mineralization. More than 430 hypogene and supergene mineral species, excluding those formed on slags, have been identified so far (for a complete list of Lavrion minerals see Wendel & Rieck 1999, Baumgaertl & Burow 2002).

Numerous outcrops of sub-economic Miocene mineralization occur within the Aegean back-arc region and especially the Attic–Cycladic belt. The area during the ancient times was a center of stone quarrying, and mining and processing of ores for the production of metals, such as copper, lead, silver and iron (Renfrew 1967, Skarpelis 2003). Skarn ores within the contact metamorphic aureoles of granitoids, carbonate replacement massive sulfides, detachment-fault related mineralization, and precious- and base-metals epithermal quartz- and barite-veins associated with steeply dipping, brittle normal faults were explored (Fig. 1) (Skarpelis 2002). Extensional tectonics favored their generation. They are part of the Tertiary–Quaternary metallogenic province in

DOI: 10.1127/0077-7757/2007/0067
0077-7757/07/0067 $ 5.75

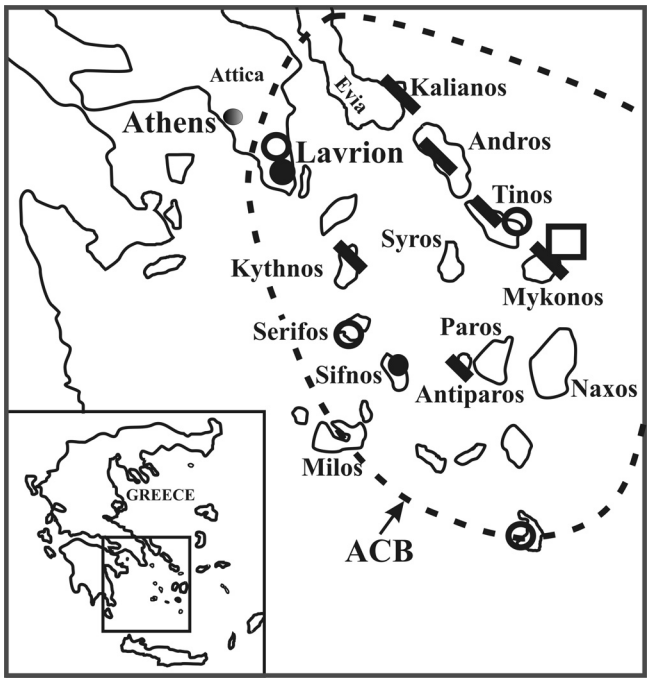

Fig. 1. Miocene ore deposit types in the Attic-Cycladic Belt (ACB) (Skarpelis 2002): carbonate replacement massive sulfides (solid circle), skarn ores (open circle), detachment-fault related mineralization (rectangular), and epithermal veins (bar).

the Aegean, which extends from the Rhodope and the Serbo-Macedonian belts in the north, to the NE Aegean islands (Lemnos, Chios, Lesbos) and Minor Asia, up to the South Aegean Active Volcanic Arc.

The geology and metallogeny of Lavrion were studied by Marinos & Petrascheck (1956). Different metallogenetic models were proposed for the Lavrion massive sulfide mineralization: replacement-type of Miocene age (Marinos & Petrascheck 1956), Lower Mesozoic syngenetic with remobilization during the granodiorite emplacement (Leleu 1966), Mississippi Valley Type (MVT) or vein Pb–Zn in calcareous rocks (Kalogeropoulos & Mitropoulos 1983).

Although Lavrion is the major Pb–Zn–Ag ore deposit in the central Aegean, a complete mineralogical study of non-skarn type primary ores, including their paragenetic sequence as well as minor elements chemistry is still lacking. Besides pure mineralogical interest, this study also aims at determining the style and the major structural controls of the mineralization in the frame of the Miocene geodynamic evolution of the Attic-Cycladic Belt. It should be considered as a necessary background for further work on the origin of the deposit. The results are compared with other occurrences of carbonate-replacement mineralization in the world.

Geological setting

Regional context

The area of Lavrion forms part of the Attic-Cycladic belt, which is composed of a stacked sequence of nappes mainly established in the Early Eocene.

In the Attic-Cycladic belt two major groups of tectonic units can be distinguished, tectonically overlying a remnant of a para-autochthonous unit (Basal Unit) (e. g. Dürr et al. 1978, Papanikolaou 1987, Schliestedt et al. 1987, Okrusch & Bröcker 1990).

a. The Basal Unit is comprised of Mesozoic platform carbonates and a Tertiary anchimetamorphic flysch (e. g. Dürr et al. 1978, Bonneau 1984). In Attica and southern Evia the para-autochthon (referred to as "Almyropotamos – Attica Unit" by Katsikatsos et al. 1986), is composed mainly of a thick sequence of Triassic-Jurrasic to middle Eocene marbles with schist intercalations (Marinos & Petrascheck 1956, Katsikatsos 1977), overlain by a metaflysch consisting chiefly of metapelites of Eocene–Oligocene age (Dubois & Bignot 1979). Glaucophane relics and Si-rich phengites in the metaflysch, demonstrate that the para-autochthon suffered a HP–LT metamorphism (~ 10 kbar/350 °C; Shaked et al. 2000). Rb–Sr dating on high–Si–phengite from mica-rich metapelites yielded c. 23 Ma ages (Ring & Reischmann 2002). These dates along with similar Rb–Sr dates on high–Si–phengite from the Basal Unit on Tinos (Bröcker & Franz 1998) and $^{40}Ar-^{39}Ar$ ages from Samos (Ring et al. 2001), were interpreted by Ring & Reischmann (2002) as the age of the high-pressure metamorphism. Bröcker et al. (2004), instead, suggested that this age constrains the timing of the greenschist facies overprint. The sedimentological, structural and metamorphic characteristics of the Basal Unit are comparable with those of the para-autochthonous Olympos Unit (e. g. Schermer et al. 1989).

b. The Lower Unit (Cycladic Blueschist Unit), dominating the Attic-Cycladic area, was thrust onto the Basal Unit. It is mainly comprised of pre-Alpine basement orthogneisses and metamorphosed Permo-Mesozoic carbonates, clastic sediments, basic and acidic volcanics and serpentinites (e. g. Dürr et al. 1978, Henjes-Kunst & Kreuzer 1982, Andriessen et al. 1987, Okrusch & Bröcker 1990). The protoliths of the Cycladic Blueschist Unit were affected by two subsequent metamorphic events: A high-pressure blueschist metamorphism during the Eocene (P ~ 12–20 kbar, T ~ 450–550 °C) (e. g. Altherr et al. 1979, 1982, Maluski et al. 1987, Matthews & Schliestedt 1984, Wijbrans &

McDougall 1986, Bröcker et al. 1993, Trotet et al. 2001 a), was followed by a medium-pressure, Barrovian overprint at the Oligocene/Miocene boundary (P ~ 5–9 kbar, T ~ 450–550 °C) (e. g. Bröcker et al. 1993, Parra et al. 2002). In the southern Cyclades (Naxos, Paros), the overprint culminated in anatectic processes and the formation of thermal domes (e. g. Jansen & Schuiling 1976, Altherr et al. 1979, 1982, Wijbrans & McDougall 1988).

U–Pb zircon geochronology of HP rocks from Syros and Tinos indicate that subduction-related processes possibly evolved from Cretaceous to Eocene (Bröcker & Enders 1999, Bröcker & Keasling 2006). Geochronology studies on zircons from high-pressure/low temperature meta-igneous lithologies from Syros, along with U–Pb ages and white mica Ar–Ar ages for the same samples support the conclusion that Eocene is the age of high-pressure metamorphism on Syros (Tomaschek et al. 2003). HP rocks are best preserved in the upper parts of the Cycladic Blueschist Unit, whereas retrogressed rock sequences predominate the lower parts of this unit (Trotet et al. 2001 b).

c. The Upper Cycladic Unit consists of non-metamorphic upper Permian to Jurassic volcaniclastics and carbonates, remnants of Eo–Hellenic ophiolites transgressively covered by upper Cretaceous limestones, and various sequences of high temperature-low pressure (HT–LP) metamorphic rocks. The HT–LP metamorphic rocks are mainly comprised of orthogneisses, amphibolites and a dismembered ophiolite. Radiometric ages of HT–LP rocks mostly indicate Late Cretaceous metamorphism (e. g. Reinecke et al. 1982, Altherr et al. 1994, Patzak et al. 1994), but indications for a Tertiary overprint were also recognized (e. g. Bröcker & Franz 1998, Zeffren et al. 2005).

Orogenic crustal-scale extension overprinted the stacked nappes. Extensional contacts operated subsequently to the overthrusting of the eclogites above the lower-grade sequences (Avigad et al. 1997 and references therein). Post-orogenic extension reworked earlier syn-orogenic thrusts and extensional contacts from the Late Oligocene until the Pliocene (Jolivet & Faccenna 2000). Studies on metamorphic core-complexes in the Cyclades suggested that back-arc extension began at least in the Early Miocene, when the Eocene HP rocks underwent the greenschist to amphibolite facies metamorphism (e. g. Lister et al. 1984, Gautier & Brun 1994, Gautier et al. 1999). Exhumation was accommodated by underthrusting of more external units and removal of overburden mainly by extension. Most structures were formed during the exhumation stage and are often associated with syn-orogenic detachments (Jolivet et al. 2003). Brichau (2004) and Brichau et al. (2006), using low-temperature thermochronology, constrained the timing and slip rates of the detachment faults in the central Aegean. The work of these authors indicates that at about 15–10 Ma, when the granites intruded, the detachment faults (brittle part of the extensional system) at Samos, Ikaria, Mykonos, Serifos and Ios started to operate, while those at Tinos and Naxos/Paros continued to remain active. Slip rates were estimated at ~ 8–7 km/Myr. Miocene extension in the Attic–Cycladic belt was accompanied by the emplacement of I- and S-type granitoids between 15–9 Ma (Altherr et al. 1982, Altherr & Siebel 2002, Pe-Piper & Piper 2002). The Cycladic islands and Lavrion became part of the magmatic arc in Late Miocene and are now in a back-arc position. Intrusion of the granitoids in the Miocene was coeval with ductile N–S to NE–SW on N-dipping detachments (e. g. Lister et al. 1984, Gautier & Brun 1994, Lee & Lister 1992). Contact metamorphic aureoles including skarns and skarn ores were developed around several intrusive bodies (Baltatzis 1981, Salemink 1985, Skarpelis & Liati 1991, Bröcker & Franz 1994).

Geology of Lavrion area

In the Lavrion area, two tectonostratigraphic Units are exposed, representing the northwestern-most continuation of the Attic-Cycladic belt: the "Basal" (para-autochthon) – possibly equivalent to lower Mesozoic marbles of the HP–LT metamorphosed Almyropotamos Unit in Evia – and the "Blueschist Unit" (allochthon, also termed as "phyllite nappe"), which is a part of the Cycladic Blueschist Belt. A detachment fault separates the Basal Unit from the Blueschists (Figs 2, 3). The original contact between them was a major thrust fault (Marinos & Petrascheck 1956, Kessel 1990 a). The detachment fault brings the Blueschist Unit into contact with the Upper and Lower marbles, the "Kaesariani schists" (Marinos & Petrascheck 1956) and their equivalent contact metamorphic rocks (this study) (Fig. 3). The rocks immediately above the detachment are cataclastically reworked mylonites (Kessel 1990 b).

The *"Basal Unit"* is comprised of metaclastic rocks ("Kaesariani schists") sandwiched between marbles ("Upper" and "Lower" marbles). On the basis of fossil findings it was concluded that sedimentation of the protoliths took place during upper Triassic–lower Jurassic times (Marinos & Petrascheck 1956). HP–LT metamorphosed granitoid bodies occur mainly within metapelites of the "Kaesariani Schists", as well as within the

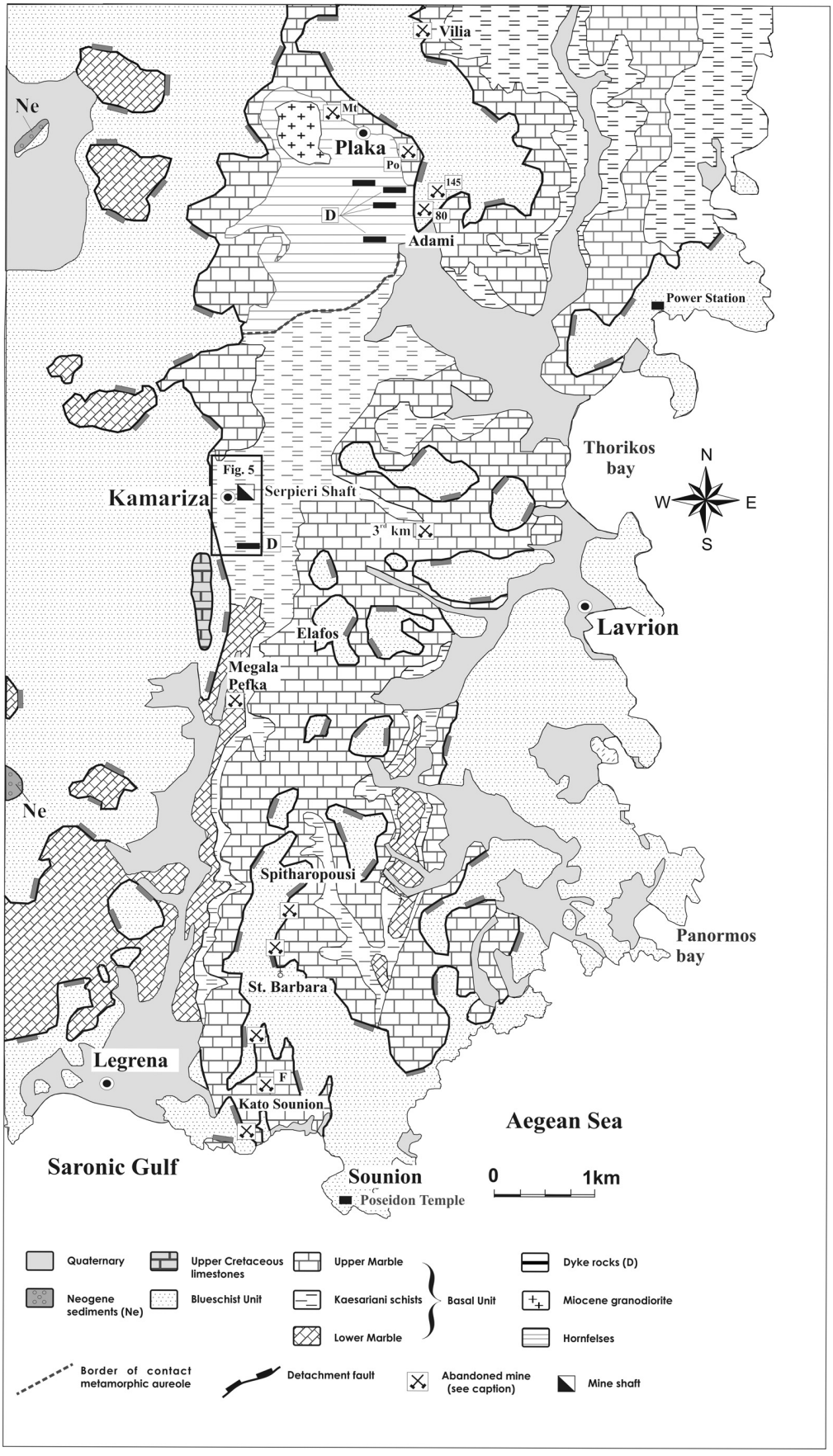

Fig. 2. Geological map of Lavrion area modified after Marinos & Petrascheck (1956), showing also abandoned mines where sampling took place (Mt: skarn type magnetite ore, Po: skarn-free carbonate-hosted pyrrhotite mineralization, F: fluorite mine; numbers of galleries indicate elevation at the adit.

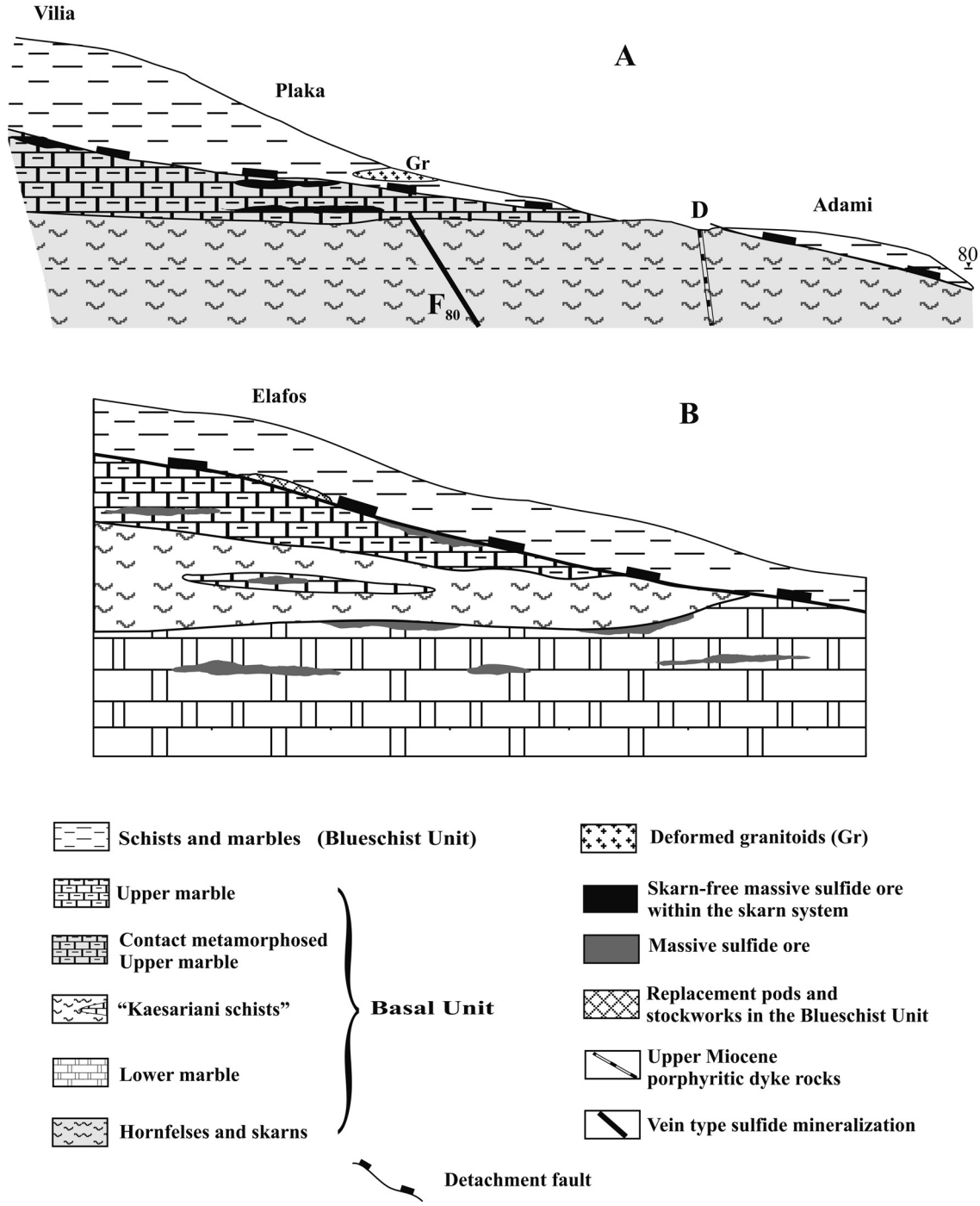

Fig. 3. Schematic graphs (not to scale) showing the tectono-stratigraphy and the geological setting of the Lavrion mineralization. **A.** Plaka area (roughly N–S, to the east of the outcrop of granodiorite stock), **B.** Elafos (W–E). Dashed line shows projection of gallery-80.

Upper marble. The marble subunits are mainly calcitic. Horizons of mica-bearing marbles are rather rare. Synfolial lenses (pods) of Mg-calcite, siderite, kutnohorite, ankerite with dispersed pyrite altered to goethite and hematite, are observed within the marble subunits (e. g. Spitharopousi, Kato Sounion). They were referred to as "ankeritized marbles" by Marinos & Petrascheck (1956), and indicate fluid channeling along mylonitic foliation planes. An early Miocene HP–LT metamorphism is assumed for the "Basal Unit" by analogy with the age and type of metamorphism of the Almyropotamos Unit in Evia.

Shear zones separate the metaclastic subunit from the footwall and hangingwall marbles. Mylonitic and cataclastic rock fabrics are observed in a narrow zone along those shear zones. As a result of intense shearing, the thickness of individual subunits varies regionally to a great extent.

The *"Blueschist Unit"* consists of HP–LT metapelites and metasandstones with minor intercalations of carbonates and blueschist metabasites retrogressed to greenschists. The metabasic rocks had experienced a progressive transformation of possibly eclogite facies rocks through epidote blueschists into greenschists (BALTATZIS 1996). Deformed granitoid bodies with penetrative structures (PAPANIKOLAOU & SYSKAKIS 1991) occur within metapelites. An Eocene age was suggested for the HP–LT metamorphic event (ALTHERR et al. 1979).

Upper Cretaceous limestones (LELEU & NEUMANN 1969), resembling stratigraphically equivalent carbonates of the Upper Cycladic Unit, and Middle Miocene lacustrine and brackish sediments (MARINOS & PETRASCHECK 1956) tectonically overlie the Blueschist Unit (Fig. 2). The former are pervasively carbonatized and silicified above the fault contact with the underlying metapelites, indicating fluid movement along that regional tectonic structure, during the late stages of ductile to brittle transition.

Miocene igneous rocks

Late brittle tectonics resulted in normal faulting of the Basal Unit, which facilitated emplacement of quartz-syenite to granite porphyries. The porphyritic rocks occur as undeformed subvertical dykes, striking WNW–ESE to WSW–ENE (Fig. 2). In the Kamariza area more than ten dykes were reported to occur, mainly underground (CAMPRESY 1889), being affected mainly by supergene alteration. A granodiorite stock intruded the Basal Unit. Intrusion of the granodiorite was accompanied by contact metamorphism of the surrounding "Kaesariani schists" (MARINOS 1937). An age of 8.27 ± 0.11 Ma by K–Ar on biotite was reported by ALTHERR et al. (1982). MARINOS (1971) obtained a K–Ar whole rock age of 8.8 ± 0.5 Ma. A fission track age of 7.3 Ma on apatite (G. WAGNER, in ALTHERR et al. 1982) indicates rapid cooling of the plutonite. The age of emplacement and the geochemical features of the Lavrion granodiorite suggest that it is a part of the Late Miocene Cycladic granitoid province (ALTHERR et al. 1982, ALTHERR & SIEBEL 2002). The granodiorite is variably altered. Sericitic hydrothermal alteration and pervasive silicification have been recognized. The orientation of the porphyritic dykes indicates a regional extensional stress field with a roughly N–S direction. It seems that the exhumation and extension of the metamorphic units was accompanied at a late stage by the intrusion first of the dykes and then the granodiorite. A tension gash array oriented WNW–ESE, with barren quartz, occurring within the hydrothermally altered sector of the granodiorite, is possibly associated with the same extensional field.

The contact metamorphic aureole

Calc-silicate hornfelses and Ca-skarns occur within the contact metamorphic aureole. Mineral assemblages in the hornfelses indicate that the protoliths were metamorphosed at temperatures between 440 and 600 °C in the presence of a H_2O-rich fluid (BALTATZIS 1981). Hornfelses were massively replaced by stratabound Ca-skarns, composed mainly of andradite-rich garnet, hedenbergitic-diopsidic clinopyroxene, hornblende, feldspar and scapolite. Epidote, actinolite, chlorite, calcite and opaques are common retrograde skarn minerals. The retrograde stage is characterized mainly by base metal sulfides and Ag-rich sulfosalts. The sharply discordant to the original bedding of the surrounding calcschists intrusive contact, along with the control of the retrograde mineral deposition by brittle structures, indicate a shallow skarn setting.

Stratabound massive magnetite to magnetite-pyrrhotite skarn ore (location marked as "Mt" on the map of Fig. 2), is developed within the Upper marble. Studies of the magnetite ore were carried out by MARINOS & PETRASCHECK (1956), LELEU et al. (1973) and ECONOMOU et al. (1981). Scheelite is dispersed within mineralized bodies and the garnetites. Massive pyrrhotite ore (Fig. 4) and base metal massive sulfide ores with pyrrhotite, being a distal expression of skarn mineralization (skarn-free replacements as defined by GILG 1996), are hosted into the Upper marble within the contact metamorphic aureole at Plaka (Fig. 3 A). Base metal sulfide ores were exploited and processed for their Zn, Pb and Ag contents. The bulk of sulfide mineralization is coincident with retrograde alteration and postdates the garnet-pyroxene formation. There is a progressive higher sulfide and lower calc-silicate gangue content of ore with increasing distance from the granodiorite stock. The Upper marble within the contact metamorphic aureole is crosscut by subvertical brittle fractures (tension gashes), which locally are mineralized with base metal sulfides and terminate at the detachment fault. The petrology of the overlying Blueschist rocks, immediately above the detachment fault, indicates that they were not affected by contact

metamorphism, nor were they attacked by the hydrothermal fluids, which gave rise to the aforementioned sulfide veinlets. Massive sulfide ores into the skarn system (e. g. at Vilia mine), located within the Upper marble close to the detachment fault, are weakly sheared (Fig. 5).

Uplift and progressive erosion of the Lavrion Units brought the ores to the surface, resulting in oxidation of the sulfides and generation of gossans. Influx into open fractures of the country rock of highly acidic metal-rich waters, owing to the oxidation of pyrite-rich sulfide protore, lead to dissolution and reprecipitation of Fe and Zn into the sequence of the host marbles, producing economically attractive Fe-ores and non-sulfide zinc deposits, which were exploited at the end of the 19th beginning of the 20th centuries (Skarpelis 2004).

Methods of investigation

Descriptions of ore bodies are based on observations in abandoned underground mines mainly in the Kamariza and Plaka mining districts (Fig. 2). Ore bodies located in an area delineated approximately by the Ilarion, Serpieri and J. Batiste shafts (Fig. 6) were sampled at Kamariza (galleries mainly on the 2nd and 3rd levels). Old mines and exploratory trenches at Vilia, Adami, Elafos, Megala Pefka, St. Barbara and Kato Sounion were additionally sampled. The mineralogy and textures of ore were studied by reflected light microscopy. Doubly polished thin sections were used for better understanding of the textural relationship between minerals. Etching by various agents was applied as well. Selected samples were investigated by Scanning Electron Microscopy using a JEOL JSM-5600 with EDX system at the Faculty of Geology & Geoenvironment, University of Athens. Accelerating voltage was 20 KV, the beam current 0.5 nA and the beam diameter < 2 µm. Natural sulfides and metal standards were used. Diffraction patterns for identification of pyrrhotite type were obtained using a Siemens D-5005 diffractometer with Cu$K\alpha$ radiation. The quartz 200 peak

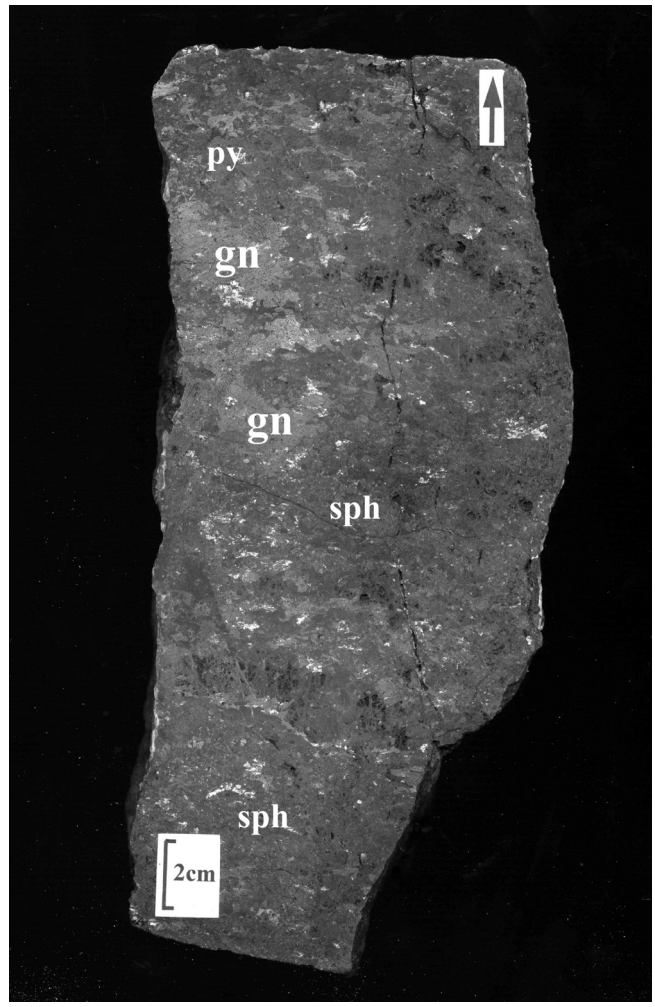

Fig. 5. Slab of Pb–Zn–Ag massive sulfide ore with shear-type deformation (Vilia mine). Arrow shows upper part of ore body (py: pyrite, gn: galena, sph: sphalerite).

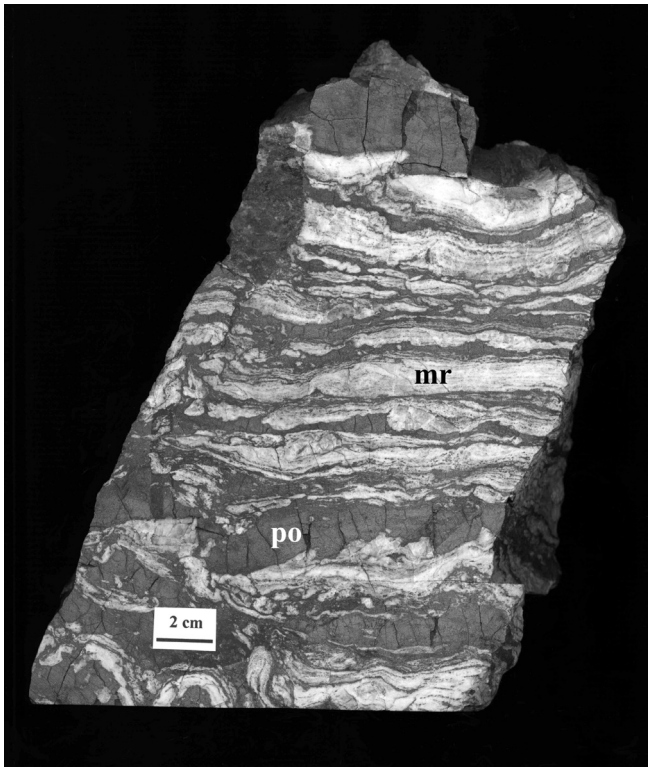

Fig. 4. Slab of stratabound pyrrhotite ore (po) into the Upper marble (mr) (Plaka).

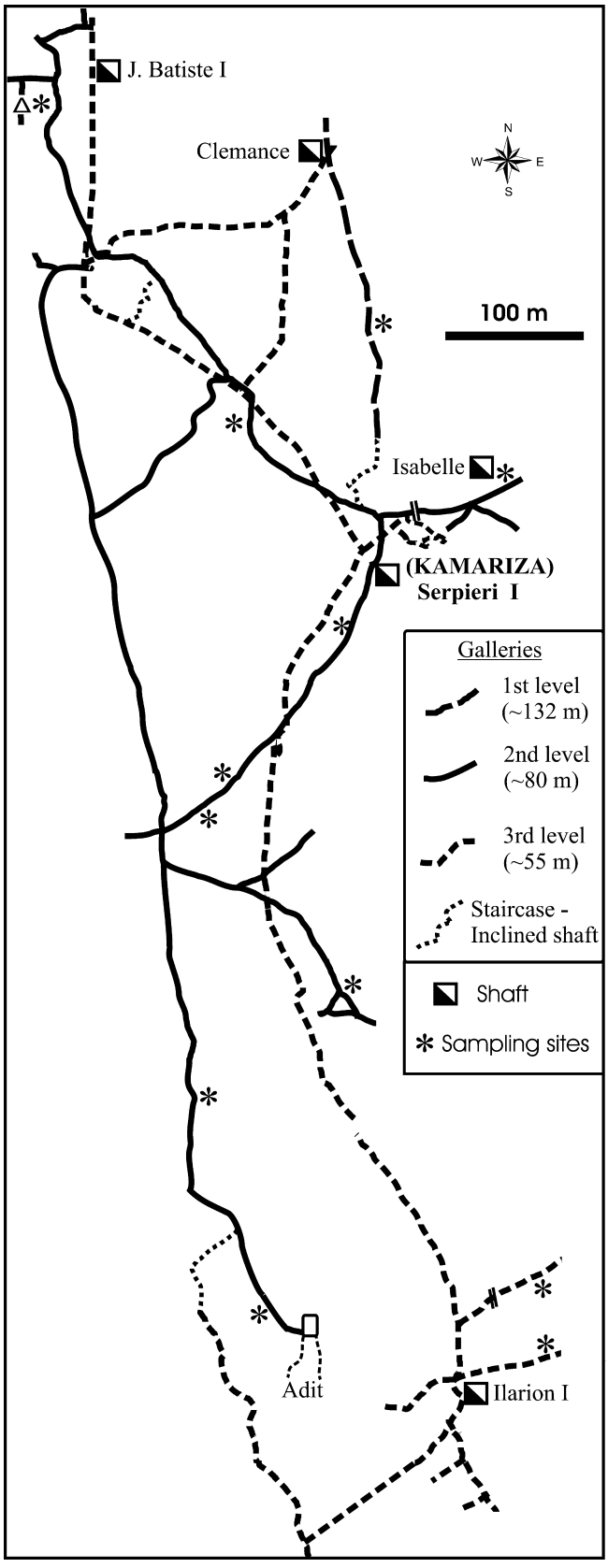

Fig. 6. Map showing sampling sites in a part of the mine workings in the Kamariza underground mine.

(2.128 Å) was used as an internal standard. It is known that the monoclinic type of pyrrhotite displays three (Tokonami et al. 1972) or four (Morimoto et al. 1975) reflections between 2.046 and 2.069 Å. The hexagonal types produce a single, sharp, symmetrical reflection at 2.065 Å. Mineral analyses were performed on a CAMECA SX50 microprobe equipped with 1 energy dispersive and 4 wavelength spectrometers at the Department of Earth and Environmental Sciences, Ludwig Maximilians University of Munich. Accelerating voltage was 15 kV and the beam current 40 nA. Natural sulfides and metals were used as standards. The beam diameter was 2 µm and the analytical software was the Xmas 4.5 from SAMx enterprise run under Windows NT. The data were reduced with the aid of the PAP algorithm. Trace elements in sphalerite and galena concentrates, as well as in bulk samples of Cu-pyrite ore were analyzed by OMAC Labs (Ireland) with Inductively Coupled Plasma Atomic Emission Spectrometry (ICP-AES) and Atomic Absorption Spectrophotometry.

Ore geometry and control

Two gross end-members of non-skarn massive sulfide ores can be distinguished: *manto-type* and *vein-type* ores.

1. Manto-type ores: Most of the Pb–Zn–Ag sulfide ore bodies bear the typical features of manto-type deposits. The thickness of the mantos varies from a few centimeters to a few meters. They occur within marbles as massive replacements. A spatial relationship of the Late Miocene porphyritic dyke rocks with the mantos is not obvious. Wall-rock alteration adjacent to sulfide ore is characterized mainly by cm-scale carbonatization, marked by precipitation of calcite, Mg-calcite, siderite and minor ankerite. Silicification of the host marble is locally observed. The marbles were decarbonatized prior to and during introduction of secondary carbonates and quartz. Tabular to sheet-like and lensoid ore bodies, as well as irregular pods are observed and are localized as follows (Fig. 3):

a. Within the two marble subunits: Ore bodies within the marbles are either partly conformable or partly cross-cutting with respect to the mylonitic foliation. They occur as synfolial lenses, as planar layers oriented parallel to the foliation plane, along shear bands of the marbles or close to/at the shear contact with the interlayered "Kaesariani schists". Relatively smaller ore bodies were explored within marble intercalations in the "Kaesariani schists" (subordinate ore). On a deposit scale these ores are both lithologically and structurally controlled. Textural relationships of the sulfides demonstrate that emp-

lacement of the mineralization was coeval with extensional deformation. Their mode of occurrence indicates that mineral deposition by hydrothermal fluids took place mainly during the transitional ductile – brittle deformation stage of the host rocks. Chimney-like ore bodies are very rare (e. g. J. Batiste mine, location marked with open triangle at top left side of Fig. 6). They are oriented at high-angle to the foliation plane of the marbles and consist of banded sulfides and quartz. They were possibly developed within faults at the stage of brittle deformation of the host rocks. The role of those faults as feeders, channeling ore fluids to favorable zones of ore deposition, is not clear since any spatial relationship with neighboring mantos is not evident.

b. Along the detachment fault: Mineralization along the detachment fault is localized predominantly in brittle structures mainly within the hangingwall carbonate beds of the Blueschist Unit (e. g. Kamariza, Elafos, Spitharopousi, St. Barbara, Kato Sounion), or into the Upper marble close to the detachment fault (e. g. "3rd Km"). Most ore bodies appear as replacement pods, stockworks and veinlets. Semimassive and disseminated sulfides occur along shear bands of carbonate rocks and usually exhibit primary undeformed textures. Stockworks of quartz and fluorite occur along tension gashes oriented perpendicular to the detachment fault. Mineralization is intensely oxidized. Close to the detachment fault a dramatic increase of hydrothermal alteration of the footwall and hangingwall rocks is observed, suggesting that hydrothermal fluids channeling along that regional tectonic structure infiltrated the fractured rocks. Hydrothermal alteration (carbonatization, minor silicification) is restricted to a narrow zone parallel to the detachment fault. It is worth mentioning that a razor-sharp contact separates non mineralized – non hydrothermally altered marbles of the Basal Unit, from mineralized hangingwall marbles and schists of the Blueschist Unit (e. g. Kato Sounion, Elafos), indicating post-mineralization slipping of the hangingwall over the footwall. The weak deformation of massive sulfide ores at Kato Sounion is possibly related to shearing along the detachment.

2. Vein-type ores: A low tonnage Ag-rich vein-type (tension gash) sulfide mineralization is hosted in hornfelses within the contact metamorphic aureole at Plaka mine (Vein F_{80}) (Fig. 3 A). The hornfelses are hydrothermally altered, revealing the vein postdates contact metamorphic phenomena. Argillic alteration assemblages, where kaolinite is the predominant clay mineral, were identified. The ore, with an overall thickness of a few decimeters, is controlled by a high-angle normal fault trending roughly WNW–ESE, dipping 40–55° SSW, being related to the Upper Miocene regional extensional stress field with roughly N–S direction. Within the contact metamorphic aureole heterolithic mineralized breccia crosscut hornfelses along high-angle fault zones.

Ore mineralogy and textures

Textures

Manto-type sulfide mineralization: The upper and lower contacts between massive sulfide ore and carbonate rock may either be razor sharp or gradational outward to disseminated. Massive sulfide ores display textures indicating wholesale replacement of marble (Fig. 7 A,

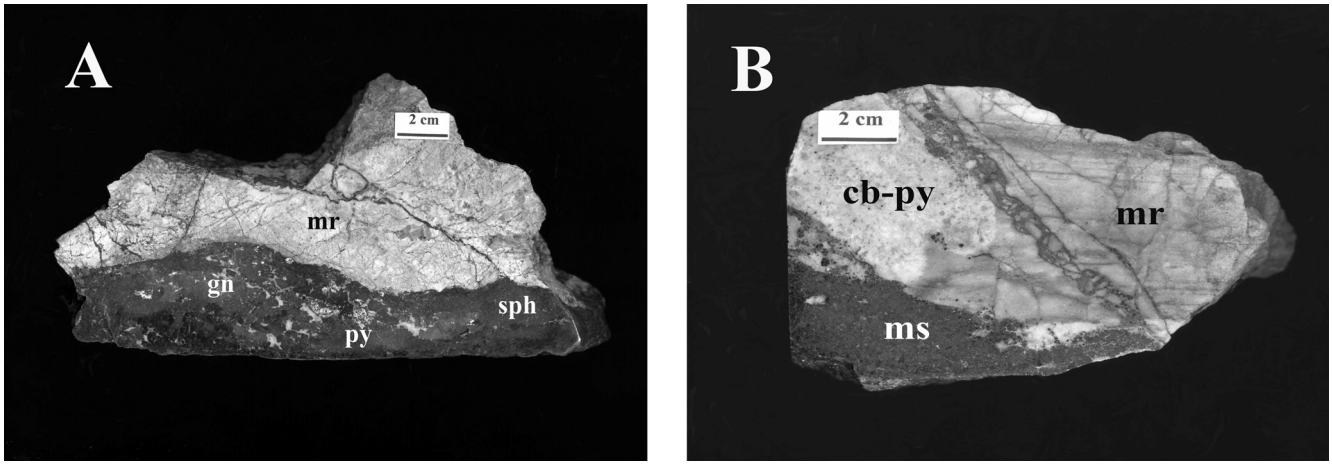

Fig. 7. A. Marble replacement by massive Pb–Zn–Ag sulfide ore (Kamariza mine). **B.** Marble replacement by sulfide ore (ms). Alteration is restricted to calcite and Mg-calcite deposition, and pyrite dispersions (cb-py). Note the mylonitic foliation of the host marble (right side) (Kamariza mine).

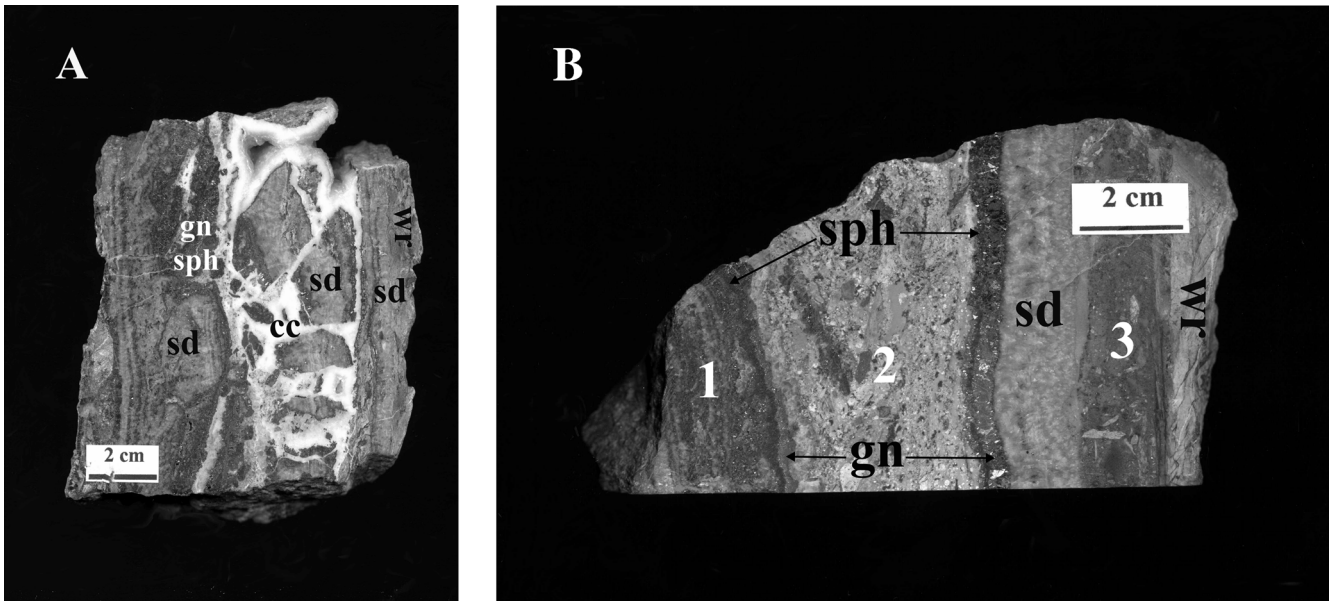

Fig. 8. A. Alternations of thin bands of sulfides and sulfosalts with bands of siderite, ankerite and fluorite. Late white calcite cements fragments of banded ore (mineralized tension gash, Plaka mine). **B.** Multiple, alternating thin bands of sulfides, sulfosalts, fluorite and siderite (1), (3); microbreccia (2) of hydrothermally altered wallrock (wr) between bands of galena and sulfosalts (gn), siderite (sd) and sphalerite (sph). (mineralized tension gash, Plaka mine). Abbreviations: marble (mr), galena (gn), pyrite (py), sphalerite (sph), carbonates (cb), massive sulfide ore (ms), siderite (sd), calcite (cc), wall rock (wr).

B) generally along mylonitic foliation or shear bands. Deposition of ore involved marble dissolution and replacement, and open space filling. The amount of open-space filling, such as incomplete infilling of voids, is minor revealing that replacement is the dominant mode of mineralization.

The ore is comprised of various proportions of sulfide minerals with a gangue dominated by carbonates (usually calcite, Mg-calcite, siderite, ankerite), fluorite, barite and quartz. Pyrite, sphalerite and galena are the major mineral constituents of most of the mantos, followed by chalcopyrite, arsenopyrite and tetrahedrite. Cupyrite ore bodies mainly consist of pyrite, arsenopyrite, chalcopyrite and minor sphalerite, galena and sulfosalts.

Ore and gangue minerals occur as granular intergrowths of varying grain size on local and ore body-wide scale. Grains of galena, sphalerite, pyrite and the gangue are commonly of a medium to coarse size. The proportions and textures of ore minerals vary widely between neighboring sulfide ore bodies and between various parts of the same ore body. The ore is mostly not deformed as can be recognized both macro- and microscopically. Textures are usually interlocking between anhedral to subhedral grains. Replacement textures are dominated by mutual embayments between individual sulfides. Most sulfosalts are intimately associated with galena, pyrite and chalcopyrite and the study of textures indicates that they were among the latest formed mineral species.

Vein-type mineralization: It has a banded appearance owing to crustification, indicating filling of open space. Alternations of thin bands of sulfide minerals and sulfosalts with bands of siderite, Mg-calcite, minor ankerite and fluorite are usual (Fig. 8 A). The ore mineral suite consists of galena, sphalerite, freibergite, tetrahedrite, pyrargyrite-proustite, pearceite-polybasite, bournonite, arsenopyrite, native silver, native arsenic, argentite and rarely stibnite and realgar. It is brecciated locally. Late calcite cementing the fragments generally is associated with native silver and realgar (Fig. 8 B).

Mineralogy

Pyrrhotite is associated with sphalerite, chalcopyrite, galena, sulfosalts and siderite in massive, skarn-free, base metal stratabound carbonate-hosted ore bodies, which occur within the contact metamorphic aureole at Plaka mine. An X-Ray Diffraction study revealed that both hexagonal and monoclinic pyrrhotite types exist, with the former predominating over the latter in most samples. Some pyrrhotite grains have been partly altered to a fine-grained mixture of pyrite and marcasite (dominantly

showing a bird's eye texture). Relictic hexagonal pyrrhotite is found in massive sulfide ores along the detachment fault (e. g. Kato Sounion). Pyrrhotite replacement by marcasite and late euhedral pyrite (Fig. 9 A), indicates increased sulfidation and perhaps more oxidized conditions over the course of time of ore formation.

Pyrite is by far the most abundant sulfide in the Lavrion deposit. It occurs as euhedral to subhedral grains that are usually embayed and replaced by sphalerite, chalcopyrite, arsenopyrite and galena, indicating most pyrite crystals were early formed. Crystal growth zoning is evident. In massive pyritic and Cu-pyritic ore bodies it shows partial replacement by chalcopyrite and smaller grain sizes in relation to the Zn–Pb-rich massive sulfide ore. *Marcasite* in the mantos occurs in minor amounts in voids and in microgeodes of massive sulfide ore. *Aikinite, emplectite* and *lilianite* occur as overgrowths or inclusions in pyrite. Minute inclusions smaller than 1 µm of a Cu–Fe–Sn sulfosalt were identified by SEM in pyrite from an ore body close to the Serpieri shaft at the 2nd level of the underground mine. Qualitative chemical analysis indicates that it is possibly stannite.

Arsenopyrite occurs in all mineralization types usually as euhedral rhomb-shaped to subhedral grains (Fig. 9 B). Arsenopyrite crystals are commonly interlocking with euhedral to subhedral pyrite and sphalerite, indicating texturally that they partly co-precipitated. Replacements of arsenopyrite by pyrite, sphalerite, chalcopyrite and galena are common. *Gersdorffite* is associated with sulfides and fluorite in semi-massive sulfide mineralization in marbles along the detachment fault (Vilia, "3rd km") and the chimney-like ore body at J. Batiste mine.

Sphalerite grains range in shape from equant and subhedral to highly irregular and embayed, replacing mainly pyrite and, to a lesser extent, chalcopyrite and arsenopyrite. Grain size ranges from several µm to several mm. Crystal growth zoning and annealing twinning are observed. Chalcopyrite disease is very common.

Galena: Galena grains in the mantos are usually subhedral to euhedral replacing mainly sphalerite, chalcopyrite and pyrite. Mutual interpenetrating boundaries between galena, sphalerite and pyrite suggest that, to some extent, they co-precipitated. Late galena in vugs and fissures within massive sulfide ore is more coarsely crystalline, usually consisting of euhedral cubic forms up to 1 cm in size. Galena from the tension gash vein-type ore in the Plaka mine forms crustiform texture in ankerite and calcite (Fig. 9 C). Inclusions of Ag-sulfosalts, native silver, native arsenic, bournonite and löllingite are common.

Chalcopyrite is abundant in the massive pyrite–arsenopyrite ore bodies, whereas it occurs in moderate abundance in the massive sphalerite-galena ones. It is interstitially developed between pyrite and chalcopyrite grains in the former or intergrown mainly with arsenopyrite, pyrite and sphalerite in the latter ore type. Inclusions of chalcopyrite in galena indicate the latter had replaced the former. Chalcopyrite rods and blebs in sphalerite occur either disseminated or commonly orientated along crystal growth zones or concentrated along cleavages and grain boundaries (chalcopyrite disease). The texture indicates that chalcopyrite has been formed later than sphalerite. Geode-like textures enclosed in chalcopyrite, usually exceeding 100 µm, are rarely found in pyritic or Cu-pyritic ore bodies. Those textures are comprised of a core of subhedral late crystals of enargite and quartz, surrounded by radial aggregates of pyrite, marcasite and barite. A rim of enargite, partly altered to covellite, is usually present (Fig. 9 D). The microscopically observed geode-like textures represent either micro-geodes or sections of mineralized microconduits for hydrothermal fluids.

Bornite is a rather rare mineral closely associated with chalcopyrite.

Fahlore is the most abundant sulfosalt in Lavrion mines. It is a minor, though widespread mineral in all ore bodies. Tetrahedrite, the dominant fahlore in the ores, and freibergite occur as anhedral grains commonly developed interstitially between sulfides. They usually occur as blebs less than 1 mm in size as well as fine disseminations in galena (Fig. 9 E, J), whereas they commonly replace chalcopyrite and sphalerite.

An enargite-luzonite polytype is interstitially developed between pyrite–chalcopyrite grains. It appears also as rims around pyrite and arsenopyrite crystals set in a chalcopyrite matrix and as veinlets in chalcopyrite. Optical properties indicate it is enargite.

Greenockite coexists with sphalerite and galena in sulfide samples unaffected by supergene processes, a fact that indicates it is hypogene (Fig. 9 F). Elsewhere in Lavrion mines greenockite appears as thin coatings and overgrowths on partly weathered sphalerite grains indicating it should be of supergene origin.

Löllingite forms radial aggregates of euhedral crystals usually less than 100 µm intergrown with galena and carbonates. Rammelsbergite was reported to occur at the mine "3rd km" by Marinos & Petrascheck (1956).

Bournonite can be fairly common in Lavrion ores as a very minor mineral constituent associated with galena and tetrahedrite (Fig. 9 J). It usually occurs as platelets in galena, preferably orientated along crystallographic planes commonly with crystal sizes < 15 µm and lamellar twins. *Lead sulfantimonites* were identified as inclusions in galena. They occur as acicular crystals or rods less

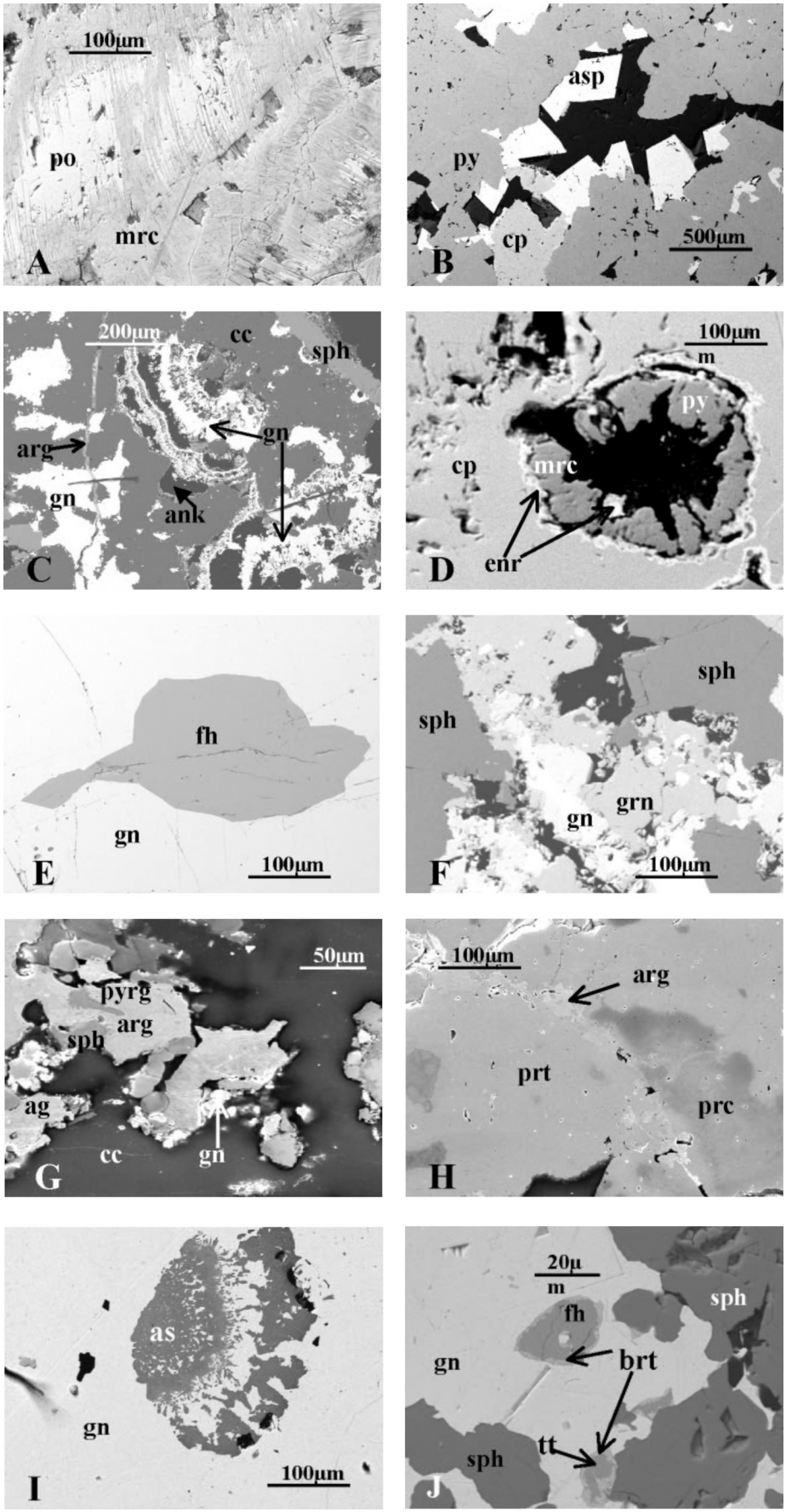

Fig. 9. BSE–EDS images of ore samples. **A.** Marcasite displaying typical lamellar texture, replacing pyrrhotite (deformed skarn-free Pb–Zn–Ag massive sulfide ore at Vilia mine; see also Fig. 5), **B.** Euhedral to subhedral open space filling arsenopyrite interlocking with pyrite and chalcopyrite (manto type ore, Kamariza mine), **C.** Microbreccia of banded galena-sphalerite ore cemented by ankerite and calcite. Late argentite filling cracks (vein-type ore, Plaka mine), **D.** Microgeode in chalcopyrite, filled with pyrite, marcasite and enargite. Thin film of enargite between pyrite – marcasite and the host chalcopyrite. Black area is polishing pit (manto type ore, Hilarion – Kamariza mine), **E.** Freibergite in galena (vein-type ore, Plaka mine), **F.** Greenockite intergrown with sphalerite and galena (vein-type ore, Plaka mine), **G.** Argentite, pyrargyrite, galena and native silver in calcitic matrix (vein-type ore, Plaka mine), **H.** Mutual intergrowths between proustite, pearceite and argentite (vein-type ore, Plaka mine), **I.** Dendritic inclusions of native arsenic in galena (vein-type ore, Plaka mine), **J.** Inclusions of freibergite, tetrahedrite and bournonite in galena (vein-type ore, Plaka mine). Abbreviations: arsenopyrite (asp), pyrite (py), sphalerite (sph), galena (gn), chalcopyrite (cp), freibergite (fh), tetrahedrite (tt), bournonite (brt), calcite (cc), ankerite (ank), argentite (arg), enargite (enr), greenockite (grn), pyrargyrite (pyrg), pyrrhotite (po), marcasite (mrc), proustite (prt), pearceite (prc), native silver (ag), native arsenic (as).

than 30 µm in length. Relics of *bismuthinite* are found in ore bodies close to the Serpieri shaft (2nd level) usually associated with bismutite and native gold.

A *silver sulfide* is intergrown with galena, pyrargyrite-proustite, iron-deficient sphalerite and carbonates (Fig. 9 G, H). It is also identified as crack-filling veinlets in galena, argentiferous tetrahedrite, proustite, pearceite and carbonates in ore samples mainly from the vein-type ore at Plaka mine. Due to the small grain size and the lack of crystallographic data, compositions within the Ag–S system in this paper are nominated as argentite.

Native silver occurs in the vein-type mineralization as massive and wire varieties in close association with Ag-rich galena (Fig. 9 G), argentite, polybasite, proustite, pearseite, iron-deficient sphalerite and late calcite. It is rather pure with traces of Au, Hg, Sb and S.

Pyrargyrite-proustite is rare and occurs as anhedral to subhedral grains closely associated with galena, pearceite–arsenpolybasite, argentite and sphalerite. In some sections it appeared to form aggregates of subhedral to anhedral crystals into a calcitic matrix.

Pearceite–arsenpolybasite is associated with pyrargyrite–proustite, galena, argentite and native silver.

Native arsenic appears as dendritic inclusions in galena in the vein ore, generally of a size ranging from 1 to 200 µm (Fig. 9 I). It also appears as botryoidal and crustiform aggregates on open cracks of carbonate minerals.

Roquesite is the first hypogene indium mineral reported from Lavrion. Rare small grains of roquesite (maximum diameter 5 µm) are intergrown with enargite and chalcopyrite in Cu-pyritic ore from ore bodies close to the Serpieri shaft.

Late-stage *realgar* from the Plaka vein-type ore is associated with calcite or *stibnite* and base metal sulfides.

Miargyrite, diaphorite, andorite, owyheeite, pyrostilpnite and *argentopyrite* had additionally been reported by Meixner & Paar (1982).

Calcite, Mg-calcite, siderite and ankerite are the dominant gangue. Euhedral crystals of carbonates (mainly calcite, siderite and ankerite), several cm in size, fill vugs in the sulfide ore. *Fluorite* is the latest mineral formed, and it is closely associated with late galena. It is a minor but persistent constituent of most of the ore bodies. It occurs as clear, white, lavender and light purple-bluish euhedral to subhedral crystals usually < 1 cm. Podiform fluorite ore bodies are found within the Upper marbles, especially at Sounion area. Euhedral to subhedral coarse fluorite (up to 5 cm) forms cockade textures or vug fills. Minor silicification associated with calcite recrystallization is observed. Fluorite as a minor mineral constituent of the vein-type mineralization at Plaka, usually occurs in the form of thin bands alternating with sulfides, sulfosalts and siderite.

Barite is usually found as euhedral platy crystals, associated with sulfides or their supergene alteration products (e. g. Vilia, Plaka). Crystal sizes up to several centimeters are common.

Apatite occurs intergrown with sulfide minerals (mainly pyrite) with grain sizes around 40 µm. The texture indicates it is not an accidental relic from the host carbonate rocks, whereas qualitative analyses indicate it is fluorapatite.

Quartz is present as euhedral and subhedral crystals in vugs and as a late formed crack filling mineral. The amount of quartz in the ore bodies is fairly less than the other gangue minerals. Euhedral quartz crystals up to 5 cm are quite rarely found. A silicification of host marbles was observed in several ore bodies. Silica replacing marble occurs locally adjacent to the mantos and never extends more than a few centimeters away from the ore contact.

Paragenetic sequence

The following simplified paragenetic mineral sequence of the manto-type mineralization (Fig. 10) is based on textural relationships. Pyrrhotite is the earliest mineral formed. Pyrite deposition commenced early and continued throughout the mineralization history, followed by arsenopyrite, sphalerite, chalcopyrite, greenockite, galena and sulfosalts. Deposition of silver-bearing minerals, other than fahlore took place late in the sequence. Fluorite, barite and quartz are among the latest hypogene minerals formed. The paragenetic sequence of the vein-type ores at Plaka (F_{80}) is roughly similar to that of mantos. The textures indicate that native silver, realgar and stibnite had been formed late in the sequence.

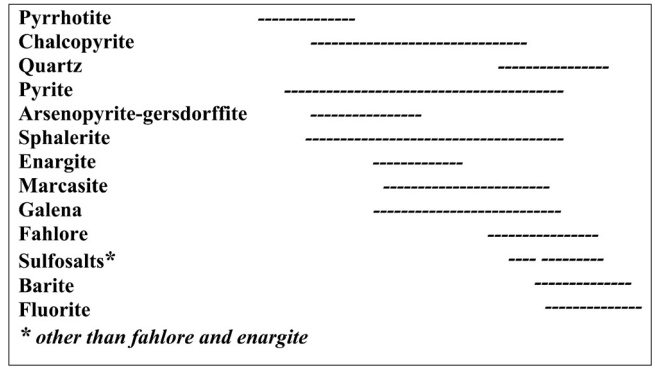

Fig. 10. Paragenetic sequence of the manto type mineralization.

Table 1. Microprobe analyses of sulfides.

Pyrrhotite[1]	mean (n = 26)	max	min	sd
Fe wt %	61.04	62.2	59.5	0.74
S	38.66	40.1	37.7	0.78
Sphalerite		mole % ZnS	mole % FeS	mole % MnS
Skarns[2]	mean (n = 50)	80.37	20.04	0.83
	sd	0.99	0.75	0.07
	max	82.88	21.64	1
	min	78.49	18.08	0.69
Mantos[3]	mean (n = 53)	86.70	12.95	0.12
	sd	2.45	2.46	0.12
	max	90.04	18.95	0.5
	min	82.95	9.91	0.01
Galena[3]	Pb*	Ag	Bi	S
mean (n = 37)	85.19	0.19	0.13	13.24
max	86.66	0.40	0.26	14.33
min	79.98	0.04	0.01	11.46
sd	1.23	0.09	0.07	0.50
Pyrite[4]	Fe	S	As	Ni
mean (n = 79)	47.03	52.66	0.64	0.01
max	48.92	54.66	2.93	0.07
min	43.18	40.87	0.03	0.01
sd	1.17	1.74	0.81	0.02
Arsenopyrite[5]	Fe	As	S	
mean (n = 22)	33.34	32.47	33.94	
max	33.82	36.46	37.11	
min	31.4	29.18	31.56	
sd	0.76	2.61	1.54	

[1] Pyrrhotite from skarn ores and skarn-free replacements (locations marked as Mt, Po, Vilia mine on Fig. 2).
[2] 80.
[3] CAR, SERP, ILA, SUB, SN.
[4] CAR, SERP, ILA, SN. [5] CAR, SERP, ILA.
* Analyses of galena, pyrite and arsenopyrite in wt %.
See Appendix for sample location and description.

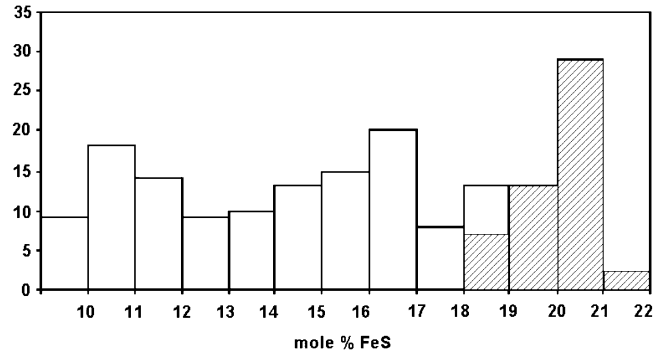

Fig. 11. Frequency distribution of sphalerite analyses from manto ores (open bars) and the pyrrhotite-sphalerite samples within the contact metamorphic aureole (diagonal).

Mineral chemistry

Electron microprobe analyses of sulfides are given in Table 1. *Pyrrhotite* of skarns and skarn-free replacements is close to the formula $Fe_{0.86-0.907}S$. Mean Ni concentration is 0.1 wt %, whereas that of Co is less than 0.01 wt %.

The mean Ni concentration of *pyrite* is low (0.01 wt %) with a range from traces to 0.05 wt %. The Co contents are uniformly low (lower than 0.01 wt %). Traces to significant concentrations of As were detected (max. value 3.5 %, mean concentration 0.64 wt %). Arsenic is negatively correlated with S, whereas the Fe content is rather constant. It is possible that As was incorporated in a metastable solid solution in the S positions or as a non-stoichiometric element as proposed by FLEET et al. (1993). Bi contents range from traces to 2.93 wt % (mean concentration 0.64 wt %).

Nearly all *sphalerite* in the ores is the high iron variety, marmatite. Electron microprobe analyses of sphalerites of 9 selected samples from manto-type ore were carried out. Sphalerites in samples of skarn-type mineralization were additionally analyzed in an attempt to assess pressure conditions of ore formation and sulfidation state. The analyses reveal that Fe is the most common element substituting for Zn. The iron content of sphalerite of the mantos varies from 9 to 19 mole% FeS. Sphalerites associated with pyrrhotite and pyrite in skarn ore yielded higher Fe (18 to 22 mole % FeS) (Fig. 11). The Mn content is low in the analyzed sphalerites (mean value 0.34 mole % MnS). Cd is distributed unevenly, in the range 0.20 to 0.58 wt %. Cu and Sn were detected in trace amounts (mean values 0.08 and 0.03 wt % respectively). The lack of critical buffer assemblage does not allow application of sphalerite geobarometry on manto ores. Sphalerites close to contacts with chalcopyrite inclusions (chalcopyrite disease) in mantos are Fe-depleted. Similar FeS depletion and texture from the Furutobe ores was interpreted as replacement of sphalerite by chalcopyrite, caused possibly by the reaction of Cu-bearing solutions and FeS in sphalerite close to chalcopyrite (BARTON 1978). Sphalerite from the vein type mineralization at Plaka is Fe-depleted (typical values in the range of 0.5 to 3 mole % FeS), far below the composition of Fe-rich sphalerite related to the mantos and the skarn ores. Application of sphalerite geobarometry to sphalerites apparently coexisting with pyrrhotite and pyrite in skarn ore, yielded unreasonably low pressures (less than 1 kbar).

Electron microprobe analyses of *arsenopyrite* of samples of manto ore from the Kamariza mine were carried out in euhedral to subhedral grains being in contact with

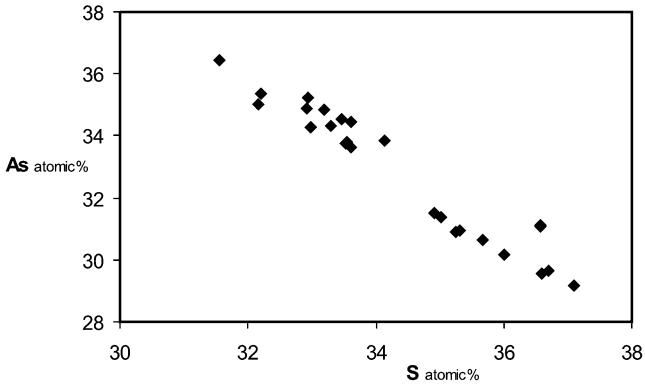

Fig. 12. Arsenic versus sulfur content (atomic %) of analyzed arsenopyrites from manto ores (Kamariza mine).

pyrite. Analyses with totals between 99.0 to 101.0 wt % and atomic % Fe in the range 33.3 ± 0.7 were accepted (Table 1). The arsenopyrites have no appreciable concentrations of elements other than Fe, As and S. The total concentration of Ni, Co and Sb in arsenopyrite does not exceed 0.1 wt %. Electron microprobe analyses indicate that no significant chemical zoning exists, with the cores showing weak As enrichment relative to the rims. Arsenic and sulfur are strongly negatively correlated following the classical substitution $FeAs_{1\pm x}S_{1\pm x}$. There is a wide range in chemical composition of arsenopyrite in terms of As (29.2 to 36.5 at.%) and S (31.6 to 37.1 at.%) (Fig. 12). Assuming deposition of arsenopyrite in equilibrium with pyrite, temperatures in the range 300 to 400 °C and fS_2 fluctuation between $10^{-7.1}$ and $10^{-10.3}$ is indicated for arsenopyrites with As at.% between 29.2 and 31.5 (Kretschmar & Scott 1976, Scott 1983, Sharp et al. 1985). Since pyrrhotite and löllingite were not identified in the arsenopyrite containing samples, it is concluded that the analyzed arsenopyrites with higher than 33.6 at.% As (Fig. 12) were not in equilibrium with existing pyrite.

Ni is substituted for Fe and Co in gersdorffite (~25 % arsenopyrite and 1 % cobaltite).

Maximum concentrations encountered by electron microprobe analysis of Ag, Bi and Sb in *galena* were 0.5, 2.33 and 0.22 at.% respectively. Analyses of patches of galena with Sb and Bi contents up to 2.5 and 3.8 wt % respectively, are possibly due to submicron size impurities of Sb- or Bi-bearing minerals. Most samples averaged 0.23 at.% Ag, 0.11 at.% Bi and 0.11 at.% Sb.

Fahlore: The first 4 analyses in Table 2 represent compositions of a fahlore inclusion in galena from the vein-type ore at Plaka mine. Since the number of Ag atoms per formula unit is higher than 3, the fahlore could be characterized as freibergite. Only traces of Pb and Te were determined. Mean at.% concentrations of Bi, Cd and Ni are 0.15, 0.04 and 0.03 respectively. The remaining analyses of fahlore in Table 2, represent tetrahedrites of various samples of manto- and vein-type ore. The calculated formula is $^{TR}(Cu, Ag)_6{}^{TET}\{Cu_{3.69-4.25}(Fe, Zn)_{1.93-2.38}\}^{SM}(As, Sb)_{3.93-4.3}S_{12.85-12.96}$, which is close to the simple stoichiometry $^{TR}(Cu, Ag)_6{}^{TET}\{Cu_4(Fe, Zn)_2\}^{SM}(As, Sb)_4S_{13}$, corresponding to an ideal structure with full occupancy of the 6 trigonal-planar (TR), 6 tetrahedral (TET) and 4 semimetal (SM) sites in the formula unit (Wuensch 1964). Cu is strongly substituted by Ag and Fe by Zn. The Ag content varies between 0.22 to 2.05 at.% whereas the As/As + Sb ratios are low (0.06 to 0.18). Significant variations in Cu/As, Sb/As and Zn/Fe ratios were not detected within single grains.

Results of electron microprobe analyses of *pyrargyrite–proustite* indicate the mineral is nearly stoichiometric, with low Cu, Fe and Zn contents. Pyrargyrite, proustite and grains of intermediate composition were determined in various samples from the vein-type mineralization at Plaka mine.

Grains of the *pearceite–arsenpolybasite* series were analyzed. By chemical analysis they can be termed pearceite or arsenpolybasite with the ratio As : Sb close to 2 : 1. It is known that pearceite–antimonpearceite and polybasite–arsenpolybasite probably form complete solid solution series. The two series are isodimorphous, with the cell dimensions of the polybasite–arsenpolybasite being double those of the pearceite–antimonpearceite series (Frondel 1963, Hall 1967). X-ray single crystal powder diffraction data cannot be obtained due to the small grain size. Thus the cell dimensions of the analysed mineral are not known. Hence, based on the chemistry of the grains, we conclude they may be pearceite or arsenpolybasite.

The analytical formula for *lead sulfantimonites* (average value is $Pb_{5.095}Sb_{3.879}S_{11.025}$) corresponds well to the ideal formula of boulangerite (a member of the *boulangerite homologous series* with the general formula Me_9S_{11}, including falkmanite, boulangerite and plumosite). Cu and As contents are negligible.

Minor amounts of Ag were detected in *bournonite* both in Kamariza and Plaka ores, possibly substituted for Cu. Micron size inclusions (< 5 µm) of an argentiferous unnamed Pb–Sb–Cu sulfosalt, were identified within bournonite.

The analyzed *Pb–Bi sulfosalt* is chemically close to the Bi-member of the incomplete solid-solution series between lillianite ($PbBi_3S_6$) and gustavite ($PbAgBi_3S_6$) of the *lillianite homologous series* as defined by Makovicky & Karup-Møller (1977).

Table 2. Electron microprobe analyses of fahlore, pyrargyrite-proustite and pearceite-arsenpolybasite (all elements in wt %).

	Sample no	Cu	Ag	Fe	Zn	As	Sb	S	Total
Fahlore/	PLK 1/1	23.8	18.7	3.2	3.6	3.5	23.4	22.9	99.1
freibergite	PLK 1/1	22.9	22.6	2.7	4.1	8.9	14.9	23.2	99.3
	PLK 1/1	22.6	21.9	3.5	3.2	5.4	19.4	23.3	99.3
	PLK 1/1	20.8	22.9	4.3	3.2	2.4	23.5	22.3	99.4
Fahlore/	PLK 145	28.6	12.9	5.3	3.1	3.6	23.1	24.2	100.8
tetrahedrite	PLK 145	31.2	9.7	4.8	3.5	3.9	23.7	23.9	100.7
	CAR 5	37.1	3.5	3.1	4.5	4.5	22.9	24.2	99.8
	SERP 3	36.6	3.5	3.4	3.6	3.8	25.6	24.8	101.3
	ILA 3	34.9	6.9	6.3	1.6	8.5	15.5	25.4	99.1
	ILA 5	37.3	3.6	3.7	3.8	8.2	16.9	25.6	99.1
				(29 atoms)					
		6.73	3.12	1.04	0.99	0.84	3.45	12.93	
		6.35	3.69	0.85	1.1	2.09	2.16	12.8	
		6.34	3.62	1.12	0.87	1.28	2.84	12.94	
		5.99	3.88	1.41	0.89	0.58	3.53	12.72	
		7.66	2.03	1.59	0.79	0.82	3.22	12.85	
		7.66	2.05	1.59	0.79	0.81	3.23	12.85	
		9.71	0.54	0.92	1.14	0.99	3.11	12.61	
		9.61	0.22	1.01	0.92	0.8	3.5	12.91	
		8.33	1.04	1.83	0.38	1.85	2.08	12.89	
		9.5	0.54	1.07	0.91	1.78	2.25	12.96	
Electron microprobe analyses of pyrargyrite-proustite									
Pyrargyrite	PLK 1/1	0.01	61.2	0.01	0.01	0.01	20.8	17.9	99.9
Intermediate	PLK 1/1	0.01	60.2	0.01	0.01	4.4	17	17.8	99.4
Proustite	PLK 1/1	0.03	66.4	0.01	0.6	13.8	0.47	19.5	100.81
	PLK 1/1	0.01	65.6	0.01	0.01	14.6	0.01	19.2	99.44
	PLK 1/1	0.01	64.6	0.01	0.01	14.9	0.8	19.5	99.83
	PLK 1/1	0.01	65.25	0.01	0.23	14.6	0.01	19.6	99.71
				(7 atoms)					
		0.01	3.06	0.01	0.01		0.92	3.01	
		0.01	2.99	0.01	0.01	0.31	0.76	2.97	
		0.01	3.03	0.01	0.04	0.91	0.02	2.99	
		0.01	3.04	0.01	0.01	0.98	0.01	2.99	
		0.01	2.97	0.01	0.01	0.99	0.03	3.01	
		0.01	3.02	0.01	0.02	0.96	0.01	3.01	
Electron microprobe analyses of pearceite-arsenpolybasite									
	PLK 1/1	7.7	68.4			5.3	4.1	15.1	100.6
	PLK 1/1	6.7	69.6			7.5	1.2	15.4	100.4
				(29 atoms)					
		2.64	13.82			1.54	0.73	10.26	
		2.28	13.95			2.17	0.21	10.39	

A minor substitution of Cu for Fe and Zn was detected in *roquesite* (up to 0.08 and 0.03 a. p. f. u. respectively).

Microprobe analyses of a diarsenide occurring as inclusions in galena indicate it is *löllingite*, displaying a minor substitution of Fe for Co and Ni (0.03 – 0.12 and 0.12 – 0.37 a. p. f. u. respectively). It is characterized by low S and Se contents and Me : As ratios indicating it is very close to the stoichiometric value.

Electron microprobe analyses of the *enargite-luzonite polytype* (Table 3) from six samples of Cu-pyritic and pyritic ore from the Kamariza mine, indicate there is very little substitution of As for Sb, and Cu for Fe, Ag and Zn. The calculated formula is: $Cu_{2.88-3.02}As_{0.98-1.09}S_4$.

Average content of Sb in *native arsenic* is 6.5 wt %.

Ore chemistry

Production data of ores exploited from various mines in Lavrion are not available. The Pb, Zn and Ag grade figures reported by Marinos & Petrascheck (1956) may

Table 3. Electron microprobe analyses of boulangerite, bournonite, lilianite, roquesite, löllingite, enargite and native arsenic (all elements in wt%).

Sample no	Cu	Ag	Pb	Sb	S	Total
			Boulangerite			
CAR 1			55.7	24.6	18.7	99
CAR 2			55.5	25.2	18.5	99.2
SUB 1			54.6	26.6	18.9	100.1
			(11 atoms)			
			5.09	3.83	11.08	
			5.09	3.93	10.97	
			4.92	4.08	11	
			Bournonite			
PLK 1	12.4	0.1	43.5	25.1	19.3	100.4
CAR 1	11.5	0.1	44.4	25.1	18.2	99.3
CAR 2	12.3	0.2	43.7	25.9	18.6	100.7
			(3 atoms)			
	0.93	0.01	1.1	1.06	2.93	
	0.93	0.01	1.1	1.06	2.92	
	0.97	0.01	1.05	1.06	2.93	
			Lilianite			
	Ag	Pb	Bi	S	Total	
SERP 10	0.4	49.5	34.4	15.8	100.1	
SERP 10a	10.2	18.7	52.7	17.6	99.2	
			(11 atoms)			
	0.04	2.92	2.01	6.02		
	1.06	1.05	2.81	6.12		
			Roquesite			
	Cu	Fe	Zn	In	S	Total
SERP 10	26.4	0.34	0.6	46.1	26.2	99.64
SERP 10a	24.9	1.6	0.3	46.2	26.4	99.4
SERP 10b	26.3	0.9	0.8	45.8	26.5	100.3
			(4 atoms)			
	1.02	0.02	0.02	0.98	2.04	
	0.95	0.08	0.01	0.98	2.02	
	1.00	0.04	0.03	0.96	2.03	
			Löllingite (n = 6)			
		Fe	Co	Ni	As	
PLK 1, 1/F	mean	18.77	1.73	7.30	71.80	
	range	16.9–20.6	0.8–3.34	3.4–10.6	70.3–72.2	
	Enargite (6 samples, n = 10, mean)				Native As (n = 13)	
CAR 3, SN 2, SERP 10, 57,		PLK 3/F	As	PLK 3/F	As	Sb
	Cu	As	S	mean	93.5	6.5
ILA 2, 3	47.5	19.4	32.54	sd	2.3	2.5
				range	91.1–97.2	2.4–11.6

well be compared with those of carbonate-hosted replacement deposits as given by Mosier et al. (1986).

Sphalerite and galena concentrates produced after chip sampling of representative mantos were analyzed during this study. Ore grade samples were crushed to appropriate sizes and then handpicked under a binocular microscope to ensure that the highest possible purity of the concentrate would be reached. Bulk samples of Cu-pyritic massive sulfide ore were additionally analyzed. The compositions of representative samples are given in Table 4. The gold content of *pyrite–arsenopyrite* concentrates from Pb–Zn–pyrite mantos ranges from 0.6 to 6 and averages 3.4 g/t. *Sphalerite* concentrates show substantial quantities of Cd. Cu contents between 0.03 to 0.1

Table 4. Elemental abundances in sphalerite and galena concentrates and bulk Cu-pyritic ore.

Sphalerite concentrates						
Sample	Zn*	Cu*	Cd	Ga	In	Sn
CAR 1	51.9	0.1	2180	22	9	56
80/1	53.3	0.09	2234	30	35	132
80/2	53.3	0.06	2258	35	17	87
PLK 145	54.2	0.05	2101	23	36	79
SERP 2/5	53.1	0.07	2245	13	34	48
ILA 3/1	50.2	0.01	2015	19	17	84
SERP 2/3	52.3	0.05	2210	16	39	104
SERP 6	55.2	0.1	2365	25	43	25
SERP 2/2	54.6	0.03	2354	23	7	95
SERP 56	52.1	0.09	2135	22	3	73

Galena concentrates				
Sample	Pb*	Bi*	Sb*	Ag
PLK 1/1	84.8	0.25	0.72	5537
PLK 1/2	82.6	0.29	0.65	4932
PLK 1/3	83.1	0.35	0.54	5754
SUB 1	82.1	0.11	0.40	2440
SUB 2	82.3	0.15	0.42	2606
ILA 3/1	81.6	0.11	0.62	2234
SERP 3/4	81.7	0.56	0.27	2375
ILA 4	82.1	0.68	0.38	2157
SUB 2	82.8	0.11	0.39	2453
SERP 3/3	82.3	0.65	0.35	2200

Chemical analyses of bulk Cu-pyritic ores

Sample	Cu*	Fe*	As*	Pb*	Zn*	Au	Ni	Sn	In	Ag	Cd
SN 1 a	3.9	27.3	20.2	0.2	0.2	5.9	242	42	35	46	621
SN 21	1.1	37.6	1.4	0.1	0.4	3.8	20	143	40	14	112
CAR 3	5.6	38.4	2.5	0.1	0.1	4.5	217	15	72	44	99
SERP 4/2	1.1	42.5	2.7	0.4	0.5	4.3	50	32	25	42	310
SERP 56	1.2	41.1	2.4	3.1	0.1	2.1	98	18	29	150	325
SERP 57	0.5	34.3	8.3	0.1	0.7	1.2	98	56	43	16	430
ILA 3	1.4	26.7	6.7	1.2	3.4	3.2	145	34	54	101	356
SUB 2	0.6	43.3	3.1	0.2	0.3	2.6	13	40	25	18	310

See Appendix for sample location and description. * in wt %; all other elements in ppm.

wt % are attributed to chalcopyrite inclusions (chalcopyrite disease). Ga, In and Sn correlate well with Zn. Ga is present in amounts between 13 to 35 ppm, In between 3 to 43 ppm, and Sn between 25 to 132 ppm. Ge contents are below the detection limit of the analytical method (2 ppm). *Galena concentrates* show substantial quantities of Ag. The silver content is proportional to the Pb grade. The highest silver value recorded is 5754 ppm (vein-type ore, Plaka mine). Antimony has been recorded in amounts up to 0.72 wt %. Bi is present in amounts between 0.11 to 0.68 wt %. Average galena compositions determined by electron microprobe were lower in Ag, Bi and Sb relative to those measured in galena concentrates, as a result of the occurrence of various mineral inclusions as described above. The *Cu-pyritic ores* have highly variable compositions in terms of As contents, mainly in the range 1.4 to 20.2 wt % and their mean As/Fe ratio is close to 0.22. Analyses of bulk samples yielded Au values between 1.2 to 5.9 g/t and low Sn and In contents. Cd ranges between 99 to 621 ppm and Ni between 13 to 242 ppm. Ga, Hg, Mo, Tl and Ge are below detection (5 ppm). Maximum recorded values for Sb, Co and Bi are 0.22, 0.01 and 0.01 wt %, respectively. Selenium was not detected at values higher than 40 ppm both in galena concentrates and in bulk Cu-pyritic samples.

Discussion and conclusions

The Lavrion deposit is the second major carbonate-hosted massive sulfide ore deposit in the Aegean, following in tonnage the Madem Lakkos and Olympias deposits in Eastern Chalkidiki. The Lavrion ores occur as replacement-style mineralization (mantos) in marbles and were mined mainly for base metals and Ag. They are structurally controlled by extensional fractures, and lithologically by the marbles. Skarn-type and especially base metal massive sulfide ore bodies within the skarn system, were of significance for their Zn, Pb and Ag contents. The genesis of the Lavrion deposit is interpreted to be related to the tectonic evolution of the area in Miocene times as a result of extensional tectonics. The close spatial relationship, at the district scale, between the manto-type ores with the detachment fault and the shear contact between the marble subunit and the "Kaesariani schists", indicates that the single most important structural control of the Lavrion mineralization is related to the large-scale back-arc Miocene extension in the Aegean. The mineralizing event obviously postdated the stage of mylonitic deformation of the host marbles, as proved by the alignment of ore bodies with the mylonitic foliation planes or by their crosscut relationship. The precise age of the manto-type of mineralization is un-

known. A Late Miocene age is indicated if the ages of regional ductile extensional shearing and the time constraints of evolution of the brittle extensional detachments in the central Aegean are considered (e. g. GAUTIER & BRUN 1994, JOLIVET et al. 2003, BRICHAU 2004, BRICHAU et al. 2006). Shearing of the skarn-free massive sulfide ores close to the detachment fault, reveals that slipping of the Blueschist Unit continued after hydrothermal activity in the Basal Unit ceased. Overall, recognition that the manto-type ore bodies show various morphologies and association with different structures within the Basal Unit and along the detachment fault (from mylonitic foliation planes to shear bands and brittle structures of the host rocks), strongly suggests that they formed continuously during extension, as the rocks were progressively carried across the transitional ductile-brittle to brittle stage. The precise temporal relationship of mantos to the skarn-type mineralization is a matter of speculation. It is obvious that the vein-type mineralization at Plaka postdates the contact metamorphic phenomena and may represent the final mineralizing event.

Mineral zonation at a district scale and in individual manto-type ore bodies is not evident. Oxidation of the ores and the lack of reliable data on bulk ore chemistry from the time of mine production, render discerning of detailed metal zoning patterns very difficult.

In addition to similarities in ore geometry and controls of the mineralization, the Lavrion ores have in common some gross textural features to other carbonate-replacement deposits in the world, like the massive replacement of carbonate rocks by sulfide mineral assemblages, the style of alteration and the minor open-space filling. The textures, the ore and gangue mineralogy as well as the chemistry of certain minerals (e. g. Fe contents in sphalerite) are comparable to those seen in other typical carbonate-replacement deposits (e. g. the North American deposits: MEGAW et al. 1988, MEGAW 1988, TITLEY 1996; the Chalkidiki deposits in northern Greece: KALOGEROPOULOS et al. 1989, GILG 1993).

The main silver carriers in the mantos are galena and fahlore. The minor modal proportion of fahlore in the ores highlights the fact that galena is the dominant silver carrier, and that the abundance of galena is the important factor in determining silver ore. The high Ag grade of the vein-filling mineralization at Plaka is mostly due to the occurrence of freibergite, silver-rich galena, argentite, native silver, pyrargyrite–proustite, pearceite–arsenpolybasite.

Elemental abundances of sphalerite and galena concentrates and of Cu-pyritic ores of manto-type mineralization indicate there are no significant enrichments in minor elements other than Cd, Ag and Au. As gold was not observed by optical and SEM microscopy in pyrite and arsenopyrite rich samples, it is concluded that either it is chemically bound in the structure of arsenopyrite and pyrite or it occurs as submicron size inclusions, thereby classifying it as "invisible" gold. Gold had never been considered a significant commodity in Lavrion, with the pyrite concentrates being used for sulfuric acid production.

The presence of pyrrhotite in the skarn zone indicates that low sulfidation state conditions prevailed during skarn ore deposition (SCOTT & BARNES 1971, EINAUDI et al. 2003).

The FeS content of sphalerite coexisting with pyrite varies continuously as a function of sulfidation state (SCOTT & BARNES 1971, CZAMANSKE 1974). Therefore the 9 to 19 mole % FeS compositions of sphalerite coexisting with pyrite in Pb–Zn–Ag mantos from Lavrion, indicate fluctuations within the field of intermediate sulfidation states, being consistent with the assemblage pyrite + chalcopyrite + tetrahedrite (EINAUDI et al. 2003). Significant local transitions to high or to very low sulfidation state are evident by the occurrence in mantos of the assemblage "enargite-pyrite + Fe-poor sphalerite" in Cu-pyritic ores, and of pyrrhotite and löllingite respectively. The transient sulfidation states may be caused by local wall rock interactions or by new pulses of sulfur-rich fluids into the ore-forming fluids (e. g. BARTON et al. 1977, EINAUDI et al. 2003).

The occurrence of low sulfidation state minerals, such as arsenopyrite and löllingite, with a mineral suite consisting of native arsenic–realgar–argentite–native silver and stibnite in the vein-type silver-rich mineralization hosted within the hornfelses at Plaka, indicates deposition from hydrothermal fluids possibly at a transition from low to intermediate sulfidation state along a cooling path.

Lavrion was indeed the most important mining and metallurgical center in the Aegean during the 5th to 4th centuries B. C. It is clear that galena, silver-carriers and possibly supergene minerals resulting from weathering were exploited and processed for the extraction of silver and lead metals. Although there has been considerable speculation, there is as yet no conclusive evidence to confirm the sources of copper and arsenic in the Aegean during the Early Bronze Age. The mineralogical and chemical features of the Lavrion mineralization indicate that ores rich in Cu and As (most probably those with a supergene mineralogical signature) should be a potential source for this metal association for the production of arsenical-copper alloy. It is further indicated that the Lavrion ores have not the suitable mineralogy and grade for processing and extraction of the Cu–Sn association.

Thus Lavrion, as suggested by Skarpelis (2003), cannot be classified into the Bronze age tin- or potential-tin sources.

Acknowledgments

Financial support by the "Special Account for Research Grants, National and Kapodistrian University of Athens" and the "Empeirikeion Foundation" is gratefully acknowledged. Part of the work on mineral chemistry was carried out during my stay with the Department of Earth and Environmental Sciences, Ludwig Maximilians University of Munich. Professor Rudolf Höll is thanked for helpful discussions and hospitality when in Munich. Professors Robert Marschik and Thomas Fehr are kindly acknowledged for making available laboratory facilities. The original manuscript benefited from constructive reviews by Dr. H. A. Gilg and Dr. M. Bröcker. Comparison of textures of Lavrion ores with those of major typical North American carbonate-replacement deposits was made possible through a collection of numerous ore and rock specimens provided by Bob Blair. The offer of Bob is gratefully acknowledged. Thanks are due to the B' Ephorate of Prehistoric and Classic Antiquities in Athens for permitting access to the Kamariza underground mine. Stathis Lazaridis, Karl Heinz Fabritz, Harry Niaschek and Rolf Wagner are thanked for their help during numerous visits of abandoned underground mines. I. Baziotis helped with drafting the maps.

References

Altherr, R., Schliestedt, M., Okrusch, M., Seidel, E., Kreuzer, H., Harre, W., Lenz, H., Wendt, I. & Wagner, G. A. (1979): Geochronology of high-pressure rocks on Sifnos (Cyclades, Greece). – Contrib. Miner. Petrol. **70:** 245–255.

Altherr, R., Kreuzer, H., Wendt, I., Lenz, H., Wagner, G. A., Keller, J., Harre, W. & Höndorf, A. (1982): A Late Oligocene/Early Miocene high temperature belt in the Attic-Cycladic crystalline complex (SE Pelagonian, Greece). – Geol. Jb. E **23:** 97–164.

Altherr, R., Kreuzer, H., Lenz, H., Wendt, I., Harre, W. & Dürr, S. (1994): Further evidence for a late Cretaceous low pressure high temperature terrane in the Cyclades, Greece. – Chem. Erde **54:** 319–328.

Altherr, R. & Siebel, W. (2002): I-type plutonism in a continental back-arc setting: Miocene granitoids and monzonites from the central Aegean Sea, Greece. – Contrib. Miner. Petrol. **143:** 397–415.

Andriessen, P. A. M., Banga, G. & Hebeda, E. H. (1987): Isotopic age study of pre-Alpine rocks in the basal units on Naxos, Sikinos and Ios, Greek Cyclades. – Geologie en Mijnbouw **66:** 3–14.

Avigad, D., Garfunkel, Z., Jolivet, L. & Azanon, J. M. (1997): Back arc extension and denudation of Mediterranean eclogites. – Tectonics **16:** 924–941.

Baltatzis, E. (1981): Contact metamorphism of a calc-silicate hornfels from Plaka area, Laurium, Greece. – N. Jb. Miner. Mh. **11:** 481–488.

Baltatzis, E. (1996): Blueschist-to-greenschist transition and the P–T path of prasinites from the Lavrion area, Greece. – Min. Mag. **60:** 551–561.

Barton, P. B. Jr. (1978): Some ore textures involving sphalerite from the Furutobe mine, Akita Prefecture, Japan. – Mining Geol. **28:** 293–300.

Barton, P. B. Jr., Bethke, P. M. & Roedder, E. (1977): Environment of ore deposition in the Creede mining district, San Juan Mountains, Colorado: Part III. Progress toward interpretation of the chemistry of the ore-forming environment. – Econ. Geol. **72:** 1–24.

Baumgaertl, U. & Burow, J. (2002): Laurion – Die Mineralien von A bis Z. – Aufschluss **53:** 278–362.

Bonneau, M. (1984): Correlation of the Hellenide nappes in the south-east Aegean and their tectonic reconstruction. – In: Dixon, J. E. & Robertson, A. H. F. (eds.): Geological Evolution of the Eastern Mediterranean. Geol. Soc. London Special Publ. **17:** 517–527.

Brichau, S. (2004): Constraining the tectonic evolution of extensional fault systems in the Cyclades (Greece) using low-temperature thermochronology. – Unpubl. Diss., Univ. Mainz 'Johannes Gutenberg" and Univ. Montpellier II, 160 pp.

Brichau, S., Ring, U., Ketcham, R. A., Carter, A., Stockli, D. & Brunel, M. (2006): Constraining the long-term evolution of the slip rate for a major extensional fault system in the central Aegean, Greece, using thermochronology. – E. P. S. L. **24:** 293–306.

Bröcker, M. & Franz, L. (1994): The Contact Aureole on Tinos (Cyclades, Greece). Part I: Field Relationships, Petrography and P–T Conditions. – Chem. Erde **54:** 262–80.

Bröcker, M. & Franz, L. (1998): Rb–Sr isotope studies on Tinos Island (Cyclades, Greece): additional time constraints for metamorphism, extent of infiltration-controlled overprinting and deformational activity. – Geol. Mag. **135:** 369–382.

Bröcker, M. & Enders, M. (1999): U–Pb zircon geochronology of unusual eclogite facies rocks from Syros and Tinos (Cyclades, Greece). – Geol. Mag. **136:** 111–118.

Bröcker, M., Bieling, D., Hacker, B. & Gans, P. (2004): High-Si phengites record the time of greenschist-facies overprinting: implications for models suggesting mega-detachments in the Aegean Sea. – J. Metamorph. Geol. **22:** 427–442.

Bröcker, M. & Keasling, A. (2006): Ionprobe U–Pb zircon ages from the high-pressure/low-temperature mèlange of Syros, Greece: age diversity and the importance of pre-Eocene subduction. – J. Metamorph. Geol. (in press).

Bröcker, M., Kreuzer, H., Matthews, A. & Okrusch, M. (1993): ^{39}Ar-^{40}Ar and oxygen isotope studies of polymetamorphism from Tinos island, Cycladic blueschist belt, Greece. – J. Metamorph. Geol. **11:** 223–240.

Campresy, A. (1889): Le Laurium. – Rev. Univ. des Mines 6, Liège, Paris.

Czamanske, G. K. (1974): The FeS content of sphalerite along the chalcopyrite – pyrite – bornite sulfur fugacity buffer. – Econ. Geol. **69:** 1328–1334.

Conofagos, K. H. (1980): The Ancient Laurium and the Greek technique for Silver production. – Ekdotiki Athinon, Athens, 458 pp.

Dubois, R. & Bignot, G. (1979): Presence d' un "hard-ground" nummulitique au sommet de la serie cretacée d' Almyropotamos (Eubée méridionale, Grèce). Conséquences. – C. R. Acad. Sci., Paris, **289 D,** 993–995.

Dürr, S., Altherr, R., Keller, J., Okrusch, M. & Seidel, E. (1978): The median Aegean crystalline belt: stratigraphy, structure, metamorphism, magmatism. – In: Cloos, H., Roeder, D. & Schmidt, K. (eds.): Alps, Apennines, Hellenides. Schweizerbart, Stuttgart, 455–476.

Economou, M., Skounakis, S. & Papathanasiou, C. (1981): Magnetite deposits of skarn type from the Plaka area of Laurium, Greece. – Chem. Erde **40:** 241–252.

Einaudi, M. T., Hedenquist, J. W. & Inan, E. E. (2003): Sulfidation State of Fluids in Active and Extinct Hydrothermal Systems: Transitions from Porphyry to Epithermal Environments. – In: Simmons, S. F. & Graham, I. (eds.): Soc. of Econ. Geol. Spec. Publ. **10:** 285–313.

Fleet, M. E., Chryssoulis, S. L., MacLean, P. J., Davidson, R. & Weisener, C. G. (1993): Arsenian pyrite from gold deposits. Au and As distribution investigated by SIMS and EMP, and colour staining and surface oxidation by XPS and LIMS. – Can. Miner. **31:** 1–17.

Frondel, C. (1963): Isodimorphism of the polybasite and pearceite series. – Amer. Miner. **48:** 565–572.

Hall, T. H. (1967): The pearceite and polybasite series. – Amer. Miner. **52:** 1311–1321.

Henjes-Kunst, F. & Kreuzer, H. (1982): Isotopic dating of prealpidic rocks from the island of Ios (Cyclades, Greece). – Contrib. Miner. Petrol. **80:** 245–253.

Jansen, J. B. H. & Schuiling, R. D. (1976): Metamorphism on Naxos: Petrology and geothermal gradients. – Am. J. Sci. **276:** 1225–1253.

Jolivet, L. & Faccenna, C. (2000): Mediterranean extension and the Africa-Eurasia collision. – Tectonics **19:** 1095–1106.

Jolivet, L., Faccenna, C., Goffé, B., Burov, E. & Acard, F. (2003): Subduction tectonics and exhumation of high-pressure metamorphic rocks in the Mediterranean orogens. – Am. J. Science **303:** 353–409.

Gautier, P. & Brun, J.-P. (1994): Crustal-scale geometry and kinematics of late orogenic extension in the central Aegean (Cyclades and Evia island). – Tectonophysics **238:** 399–424.

Gautier, P., Brun, J.-P., Moriceau, R., Sokoutis, D., Martinod, J. & Jolivet, L. (1999): Timing, kinematics and cause of Aegean extension: a scenario based on comparison with simple analogue experiments. – Tectonophysics **315:** 31–72.

Gilg, H. A. (1993): Geochronological (K-Ar), fluid inclusion and stable isotope (C, H, O) studies of skarn, porphyry copper, and carbonate-hosted Pb–Zn (Ag, Au) replacement deposits in the Kassandra mining district (Eastern Chalkidiki, Greece). – Unpubl. Diss., E. T. H. Zurich, 153 pp.

Gilg, H. A. (1996): Fluid inclusion and isotope constraints on the genesis of High-Temperature Carbonate-Hosted Pb–Zn–Ag Deposits. – In: Sangster, D. F. (ed.): Carbonate-hosted Lead-Zinc Deposits, Soc. of Econ. Geol. Spec. Publ. No **4:** 501–514.

Kalogeropoulos, S. & Mitropoulos, P. (1983): Fluid inclusion characteristics of fluorite from Laurium (Greece). – Ann. Geol. Pays Hell. **31:** 130–135.

Kalogeropoulos, S. I., Kilias, S. P., Bitzios, D. C., Nikolaou, M. & Both, R. A. (1989): Genesis of the Olympias carbonate-hosted Pb–Zn (Ag–Au) sulfide ore deposit, eastern Chalkidiki peninsula, northern Greece. – Econ. Geol. **84:** 1210–1234.

Katsikatsos, G. (1977): La structure tectonique d' Attique et de l' île d' Eubée. – In: Kallergis, G. (ed.): Proc. of the VI Colloquium on the Geology of the Aegean Region. I. G. M. R., Athens **1:** 211–228.

Katsikatsos, G., Migiros, G., Triantafyllis, M. & Mettos, A. (1986): Geological structure of Internal Hellenides (E. Thessaly – SW Macedonia, Euboea – Attica – Northern Cyclades Islands and Lesbos). – Geol. & Geoph. Res., Spec. Issue, I. G. M. E., Athens, 191–212.

Kessel, G. (1990 a): Attic Peninsula (Greece): Deformation and P-T path of the Crystalline Units. – In: Savascin, M. Y. & Eronat, A. H. (eds.): IESCA 1990, Internat. Earth Sciences Congress on Aegean Regions, Izmir **1:** 258–260.

– (1990 b): Untersuchungen zur Deformation und Metamorphose in Attischen Krystallin, Griechenland. – Berliner Geowissenschaftl. Abh. A **126:** 1–150.

Kretschmar, U. & Scott, S. D. (1976): Phase relations involving arsenopyrite in the system Fe–As–S and their application. – Can. Miner. **14:** 364–386.

Lee, J. & Lister, G. (1992): Late Miocene ductile extension and detachment faulting, Mykonos, Greece. – Geology **20:** 121–124.

Leleu, M. (1966): Les gisements plombo-zincifres du Laurium (Grèce). – Sciences de la Terre XI, **3:** 293–343.

Leleu, M. & Neumann, M. (1969): L' âge des formations d' Attique: du paleozoique au mesozoique. – C. R. Acad. Sci., Paris **268:** 1361–63.

Leleu, M., Morikis, A. & Picot, P. (1973): Sur des mineralizations de type skarn au Laurium (Grece). – Miner. Deposita **8:** 259–263.

Lister, G. S., Banga, G. & Feenstra, A. (1984): Metamorphic complexes of Cordilleran type in the Cyclades, Aegean Sea, Greece. – Geology **12:** 221–225.

Maluski, H., Bonneau, M. & Kienast, J. R. (1987): Dating the metamorphic events in the Cycladic area: $^{39}Ar/^{40}Ar$ data from metamorphic rocks of the island of Syros (Greece). – Bull. Soc. Geol. France **5**, III: 833–842.

Makovicky, E. & Karup-Möller, S. (1977): Chemistry and crystallography of the lilianite homologous series. I. General properties and definitions. – N. Jb. Miner. Abh. **130:** 264–287.

Marinos, G. (1937): The granite of Plaka and the associated contact metamorphism (Lavreotiki penisnula). – Unpubl. Diss., Univ. of Athens (in Greek), 52 pp.

Marinos, G. P. (1971): On the radiodating of Greek rocks (In Greek, English summary). – Ann. Geol. Pays Hell. **23:** 175–182.

Marinos, G. P. & Petrascheck, W. E. (1956): Lavrion. Institute for Geology and Subsurface Research, Geol. & Geoph. Res. 4, **1:** 1–247.

Matthews, A. & Schliestedt, M. (1984): Evolution of the blueschist and greenschist facies rocks of Sifnos, Cyclades, Greece. – Contrib. Miner. Petrol. **88:** 150–163.

Meixner, H. & Paar, W. (1982): New Observations on Ore Formation and Weathering of the Kamariza Deposit, Laurium, SE Attica (Greece). – In: Amstutz, G. C., Goresy, A. E., Frenzel, G., Kluth, C., Moh, G., Wauschkuhn, A. & Zimmermann, R. A. (eds.): Ore Genesis; The State of the Art. Springer-Verlag, Berlin, Heidelberg, New York, 760–767.

Megaw, P. K. M. (1988): Tectonic localization and controls on High-Temperature, Carbonate-Hosted Ag–Pb–Zn Deposits of Mexico. – In: Kisvarsanyi, G. & Grant, S. K. (eds.): Proc. "North American Conference on Tectonic Control of Ore Deposits and the Vertical and Horizontal Extend of Ore Systems, Univ. of Missouri-Rolla, 92–102.

Megaw, P. K. M., Ruiz, J. & Titley, S. R. (1988): High-Temperature, Carbonate-Hosted Ag–Pb–Zn(Cu) deposits of Northern Mexico. – Econ. Geol. **83:** 1856–1885.

Morimoto, N., Gyobu, A., Mukaiyama, H. & Izawa, E. (1975): Crystallography and stability of pyrrhotites. – Econ. Geol. **70:** 824–833.

Mosier, D. L., Morris, H. T. & Singer, D. A. (1986): Grade and tonnage model of polymetallic replacement deposits. – In: Cox, D. P. & Singer, D. A. (eds.): Mineral Deposit Models: U. S. Geol. Survey Bull. **1693:** 101–104.

Okrusch, M. & Bröcker, M. (1990): Eclogite facies rocks in the Cycladic blueschist belt, Greece: A review. – Eur. J. Miner. **2:** 451–478.

Papanikolaou, D. (1987): Tectonic evolution of the Cycladic blueschist belt (Aegean sea, Greece). – In: Helgeson, H. C. (ed.): Chemical Transport in Metasomatic Processes, Reidel Publishing Company, Dordrecht, 429–450.

Papanikolaou, D. & Syskakis, D. (1991): Geometry of acid intrusives in Plaka, Laurium and relation between magmatism and deformation. – Bull. Geol. Soc. Greece **25,** 1: 355–368.

Parra, T., Vidal, O. & Jolivet, L. (2002): Relation between the intensity of deformation and retrogression in blueschist metapelites of Tinos Island (Greece) evidenced by chlorite-mica local equilibria. – Lithos **63:** 41–66.

Patzak, M., Okrusch, M. & Kreuzer, H. (1994): The Akrotiri unit on the island of Tinos, Cyclades, Greece: Witness to a lost terrane of Late Cretaceous age. – N. Jb. Geol. Paläont. Abh. **194:** 211–252.

Pe-Piper, G. & Piper, D. (2002): The igneous rocks of Greece: anatomy of an orogen. – Beitrage z. Regionalen Geol. der Erde, Gebr. Borntraeger, Berlin, Stuttgart.

Renfrew, C. (1967): Cycladic Metallurgy and the Aegean Early Bronze Age. – Aegean J. Archaeol. **71:** 1–20.

Reinecke, T., Altherr, R., Hartung, B., Hatzipanagiotou, K., Kreuzer, H., Harre, W., Klein, H., Keller, J., Geenen, E. & Böger, H. (1982): Remnants of a Late Cretaceous high temperature belt on the island of Anafi (Cyclades, Greece). – N. Jb. Miner. Abh. **145:** 157–182.

Ring, U. & Reischmann, T. (2002): The weak and superfast Cretan detachment, Greece: exhumation at subduction rates in extruding wedges. – J. Geol. Soc. London **159:** 225–228.

Ring, U., Layer, P. W. & Reischmann, T. (2001): Miocene high-pressure metamorphism in the Cyclades and Crete, Aegean Sea, Greece: Evidence for large-scale magnitude displacement on the Cretan detachment. – Geology **29:** 395–398.

Salemink, J. (1985): Skarn and ore formation at Seriphos, Greece. – Unpubl. Diss., Geol. Ultraiectina **40:** 1–231.

Schermer, E. R., Lux, D. & Burchfield, B. C. (1989): Age and tectonic significance of metamorphic events in the Mt. Olympos region, Greece. – Bull. Geol. Soc. Greece **23:** 13–27.

Schliestedt, M., Altherr, R. & Matthews, A. (1987): Evolution of the Cycladic Crystalline Complex: petrology, isotope geochemistry and geochronology. – In: Helgeson, H. C. (ed.): Chemical Transport in Metasomatic Processes, Reidel Publishing Company, Dordrecht, 76–94.

Scott, S. D. (1983): Chemical behaviour of sphalerite and arsenopyrite in hydrothermal and metamorphic environments. – Min. Mag. **47:** 427–435.

Scott, S. D. & Barnes, H. I. (1971): Sphalerite geothermometry and geobarometry. – Econ. Geol. **66:** 653–669.

Shaked, Y., Avigad, D. & Garfunkel, Z. (2000): Alpine high-pressure metamorphism at the Almyropotamos window (southern Evia, Greece). – Geol. Mag. **137:** 367–380.

Sharp, Z. D., Essene, E. J. & Kelly, W. C. (1985): A re-examination of the arsenopyrite geothermometer: Pressure considerations and applications to natural assemblages. – Can. Miner. **23:** 517–534.

Skarpelis, N. (2002): Geodynamics and evolution of the Miocene mineralization in the Cycladic – Pelagonian belt, Hellenides. – Bull. Geol. Soc. Greece **34,** 6: 2191–2206.

Skarpelis, N. (2003): Ancient potential tin sources in the Aegean. – In: Giumlia-Mair, Al. & Lo Schiavo, Fl. (eds.): The Problem of Early Tin, British Archaeological Reports International Series **1199:** 159–164.

Skarpelis, N. (2004): Geology and origin of supergene iron and zinc ores at Lavrion, Attica (Greece). – 10th Congress Geol. Soc. Greece, Thessaloniki, 590–591.

Skarpelis, N. & Liati, A. (1990): The prevolcanic basement of Thera at Athinios: Metamorphism, Plutonism and Mineralization. – In: Hardy D. A. (ed.): Thera and the Aegean World III, The Thera Foundation 2, 172–182, London.

Titley, S. R. (1996): characteristics of High Temperature, Carbonate-hosted replacement ores and some comparisons with Mississippi Valley-Type ores. – In: Sangster, D. F. (ed.): Carbonate-Hosted Lead-Zinc Deposits. Society of Economic Geologists Spec. Publ. **4:** 244–254.

Tokonami, M., Nishiguchi, K. & Morimoto, N. (1972): Crystal structure of a monoclinic pyrrhotite. – Amer. Miner. **57:** 1066–1080.

Tomaschek, F., Kennedy, A. K., Villa, I. M., Lagos, M. & Ballhaus, C. (2003): Zircons from Syros, Cyclades, Greece – Recrystallization and Mobilization of Zircon During High-Pressure Metamorphism. – J. of Petrol. **44,** 11: 1977–2002.

Trotet, F., Vidal, O. & Jolivet, L. (2001 a): Exhumation of Syros and Sifnos metamorphic rocks (Cyclades, Greece). New constraints on the *P–T* paths. – Eur. J. Miner. **13:** 901–920.

Trotet, F., Jolivet, L. & Vidal, O. (2001 b): Tecto-no-metamorphic evolution of Syros and Sifnos islands (Cyclades, Greece). – Tectonophysics **338:** 179–206.

Wijbrans, J. R. & McDougall, I. (1986): $^{40}Ar/^{39}Ar$ dating of white micas from an Alpine high-pressure belt on Naxos (Greece): resetting of the argon isotopic system. – Contrib. Miner. Petrol. **93:** 187–194.

Wijbrans, J. R. & McDougall, I. (1988): Metamorphic evolution of the Attic-Cycladic Metamorphic Belt on Naxos (Cyclades, Greece) utilizing $^{40}Ar/^{39}Ar$ age spectrum measurements. – J. metamorphic Geology **6:** 571–594.

Wendel, W. & Rieck, B. (1999): Lavrion: Die komplette Mineralliste. – Lapis **24** (7–8): 61–67.

Wuench, B. J. (1964): The crystal structure of tetrahedrite, $Cu_{12}Sb_4S_{13}$. – Z. Krist. **19:** 437–453.

Zeffren, S., Avigad, D., Heimann, A. & Gvirtzman, Z. (2005): Age resetting of hanging wall rocks above a low-angle detachment fault: Tinos Island (Aegean Sea). – Tectonophysics **400:** 1–25.

Appendix: Sample location and description.

Sample Code	Sample location (see Figs. 2, 6)	Description
CAR	Along the gallery from the adit to the Serpieri I shaft – 2nd mining level	Massive sulfide ores (mantos) within the Lower Marble
SUB	Along the gallery from the adit to the Serpieri I shaft – 2nd mining level	Massive sulfide ore within marble intercalation into the "Kaesariani schists" ("subordinate ore")
SERP	Various sites between the J. Batiste, Clemance and Isabelle shafts (2nd and 1st mining levels)	Massive sulfide ores (mantos) within the Lower Marble
ILA	Various sites to the NE of the Ilarion shaft – 3rd mining level	Massive sulfide and disseminated ores (mantos) within the Lower Marble
SN	Kato Sounion (mines 7, 12)	Massive sulfide ores (mantos) along the detachment fault
80	Gallery 80	Massive skarn ore (mt, po, base metal sulfides)
PLK 145	Gallery 145	Massive Zn–Pb–Ag ore – skarn-free replacements within the skarn system
PLK 1	Vein 80 (F_{80}) (located to the west of gallery 80, approximately 550 m to the north of the adit of the gallery)	Banded vein-type sulfide ore within the hornfelses

Received: April 18, 2006; accepted: September 18, 2006

Responsible editor: R. Klemd

Authors' address:

Dr. Nikos Skarpelis, Faculty of Geology & Geoenvironment, Department of Economic Geology & Geochemistry, University of Athens, Panepistimiopoli, 15784 Zografou, Athens, Greece.
e-mail address: skarpelis@geol.uoa.gr